

Published in final edited form as:

*Proteomics Clin Appl.* 2009 ; 3(10): 1151–1173. doi:10.1002/prca.200900043.

## Toward the Proteome of the Human Peripheral Blood Eosinophil

Christof Straub<sup>1</sup>, Konrad Pazdrak<sup>1</sup>, Travis W. Young<sup>1,4</sup>, Susan J. Stafford<sup>3</sup>, Zheng Wu<sup>1,3</sup>, John E. Wiktorowicz<sup>1,2,3</sup>, Anthony M. Haag<sup>3</sup>, Robert D. English<sup>3</sup>, Kizhake V. Soman<sup>1,2,3</sup>, and Alexander Kurosky<sup>1,2,3</sup>

<sup>1</sup>Department of Biochemistry and Molecular Biology, University of Texas Medical Branch, Galveston, TX, USA

<sup>2</sup>The UTMB NHLBI Proteomics Center, University of Texas Medical Branch, Galveston, TX, USA

<sup>3</sup>The UTMB Biomolecular Resource Facility, University of Texas Medical Branch, Galveston, TX, USA

### Abstract

Eosinophils are granular leukocytes that have significant roles in many inflammatory and immunoregulatory responses, especially asthma and allergic diseases. We have undertaken a fairly comprehensive proteomic analysis of purified peripheral blood eosinophils from normal human donors primarily employing 2-dimensional gel electrophoresis with protein spot identification by matrix-assisted laser desorption/ionization mass spectrometry. Protein subfractionation methods employed included isoelectric focusing (Zoom<sup>®</sup> Fractionator) and subcellular fractionation using differential protein solubilization. We have identified 3,141 proteins which had Mascot expectation scores of  $10^{-3}$  or less. Of these 426 were unique and non-redundant of which 231 were novel proteins not previously reported to occur in eosinophils. Ingenuity Pathway Analysis showed that some 70% of the non-redundant proteins could be subdivided into categories that are clearly related to currently known eosinophil biological activities. Cytoskeletal and associated proteins predominated among the proteins identified. Extensive protein posttranslational modifications were evident, many of which have not been previously reported that reflected the dynamic character of the eosinophil. This dataset of eosinophilic proteins will prove valuable in comparative studies of disease *versus* normal states and for studies of gender differences and polymorphic variation among individuals.

### Keywords

Asthma; 2-DE; Eosinophils; Phosphoproteins; Protein expression

### 1 Introduction

Eosinophils are pleiotropic multifunctional granulocytic leukocytes that function in diverse inflammatory and immunoregulatory responses [see reviews 1, 2]. Important pathologies associated with eosinophils include asthma, allergy, and parasitic helminth infections [1, 3]. In normal adults eosinophils are produced, differentiated, and matured in the bone marrow, migrate into the peripheral blood, and subsequently target to different tissues including mammary gland, thymus, uterus, lung, and especially the gastrointestinal tract [1]. However,

**Correspondence:** Dr. Alexander Kurosky, Department of Biochemistry and Molecular Biology, The University of Texas Medical Branch, 301 University Blvd., Galveston, TX 77555-0635, USA, akurosky@utmb.edu, **Fax:** +1-409-772-8025.

<sup>4</sup>Currently at the Center for Technology Development, Texas A&M University, College Station, TX, USA

**Conflict of interest** - The authors have no financial conflict of interest.

in many inflammatory pathologies eosinophils can also be associated with numerous other organs and tissues. Eosinophil trafficking into inflammatory sites involves a number of cytokines, chemokines, growth factors, lipids, as well as four major cationic proteins (EPO, MBP, ECP, EDN) packaged within four types of cytoplasmic granules each with unique morphologies [1-4].

Most current established methods of preparing eosinophils from peripheral blood utilizing anti-CD16 immunomagnetic beads to remove neutrophils yield a population of cells which is relatively homogenous typically greater than 98% [5]. However, density gradient centrifugation can further distinguish two populations of eosinophils termed “normodense” (specific gravity > 1.085 g/l) and “hypodense” (specific gravity < 1.085 g/l) [6]. Hypodense eosinophils typically account for 5–10% of the total peripheral blood eosinophil population in normal adults and represent activated and degranulated cells [7]. Normodense eosinophils can be converted to a hypodense form *in vitro* by a number of different stimuli; e.g., GM-CSF, IL-3, eotaxin and IL-5 [8]. Moreover, in many inflammatory pathologies the hypodense population of cells is increased; however, the composition of these hypodense eosinophils can differ when compared with *in vitro* stimulated cells [4, 8-9]. Therefore, within the hypodense population of eosinophils there is indication of further microheterogeneity likely due to differential degranulation depending on the nature of the stimulus employed or the pathology involved. Thus, the molecular basis for all of the observed eosinophil heterogeneity is not fully established and clearly requires further investigation. A comparative proteome map of eosinophils from normal adults would be considerably important toward defining eosinophil heterogeneity, especially in inflammatory diseases.

It is clear that eosinophils play an important role in the etiology of bronchial asthma which is one of the fastest growing diseases in the Western world. The prevalence of asthma has increased steadily over the last two decades and in 2006 an estimated 16.1 million adults (7.3% > 18 y) and some 9.4% or 6.8 million children were affected by the disease in the United States [10]. The rapid increase in the incidence of asthma and its resulting consequence on the healthcare system underscores the need for the identification of new therapeutic targets for the treatment of allergic inflammation. None of the currently available treatments for asthma and allergic diseases are curative. Recently, a number of factors have been proposed which appear to control eosinophil trafficking, survival and activation in animal models; however, to date, no therapeutic target has been developed which successfully eliminates tissue-activated eosinophils in human trials. Furthermore, the dual role of eosinophils in pro-inflammation and anti-inflammation has yet to be elucidated fully. Together these findings clearly emphasize the current status of an incomplete understanding of eosinophil activation and function, and argue for more comprehensive studies of the eosinophil phenotype.

We hypothesize that an unbiased characterization of a comprehensive set of proteins expressed by eosinophils will provide novel insights into the molecular circuitry, signaling pathways, proinflammatory mediators and cytokines that may play a role in the pathogenesis of eosinophil inflammation. Furthermore, the map will be important in comparative eosinophil studies of disease or therapeutic treatments. In the present work we initiated the proteomic characterization of peripheral blood eosinophils obtained from healthy, non-allergic donors. Furthermore, in order to decrease the complexity of the cell lysate and maximize the total number of proteins identified in the study, we fractionated the cell lysate into cytoplasmic, membrane, organelle, granule, and nuclear fractions, and resolved the proteins by 2-DE. We report a number of proteins that are unique to eosinophils and are associated with eosinophil effector functions. We posit that the present data will therefore serve as an important reference database for the discovery of markers of activated eosinophils and for future studies investigating therapeutic targets for eosinophilia-related inflammatory diseases.

## 2 Materials and Methods

### 2.1 Materials

Histopaque<sup>®</sup>-1077,  $\alpha$ -cyano-4-hydroxycinnamic acid, benzamidine, leupeptin, aprotinin, microcystin, and dextran (Fluka) were obtained from Sigma-Aldrich (St. Louis, MO). Sodium orthovanadate and PMSF were products of Fisher Scientific (Fair Lawn, NJ). Thiourea, CHAPS, iodoacetamide, IPG strips (pH 5–8), Precision Plus molecular weight standards, Protean II XL Tris-HCL precast gels (8–16%), Criterion Tris-HCl precast gels (8–16%), RC DC protein assay kit (Lowry method with reduction compatibility (RC) and detergent compatibility (DC), Criterion Dodeca electrophoretic 13.3 cm  $\times$  8.7 cm multi-gel cell (12 gels, 11 cm strips) and Protean II XL electrophoretic 19.3 cm  $\times$  18.3 cm cell (2 gels, 18 cm strips) were products from BioRad (Hercules, CA.). IPG strips (11 and 18 cm, pH 3–10, 4–7, and 6–11), DeStreak rehydration buffer, IPG buffer/ampholytes, and Ettan DALT IPGphor II isoelectric focusing cell were obtained from GE Healthcare. TCEP and Perfect-FOCUS (protein precipitation reagent for 2-DE samples) were purchased from G-Biosciences (St. Louis, MD). Sypro Ruby fluorescent protein gel stain, Pro-Q Diamond fluorescent phosphoprotein gel stain, Peppermint Stick phosphoprotein molecular weight markers, and a Zoom<sup>®</sup> IEF fractionator were obtained from Invitrogen (Carlsbad, CA). HBSS without Mg<sup>2+</sup> or Ca<sup>2+</sup> was from Gibco. The ProteoExtract<sup>®</sup> Subcellular Proteome Extraction kit was from Calbiochem (San Diego, CA). VarioMACS separation columns, MACS Separator (magnetic), and CD16 MicroBeads for eosinophil isolation were purchased from Miltenyi Biotec (Auburn, CA).

### 2.2 Eosinophil isolation from peripheral human blood

Blood donors for eosinophil isolation included three female and five male non-smoking donors (ages 18–50 y) who showed neither asthmatic nor allergic symptoms [5]. Briefly, 1.5 ml of 15% Dextran and 1.5 ml of 0.25 M EDTA was immediately added to 60 ml of collected blood in two 50 ml polypropylene conical centrifuge tubes and allowed to sediment for 30 min at RT. After sedimentation, the leukocyte-containing layer was overlaid onto Histopaque<sup>®</sup>-1077 (15 ml leukocyte/7.5 ml Histopaque<sup>®</sup> and centrifuged (720  $\times$  g) at RT for 40 min. Following washing at 4°C with 20 mM HEPES-1X HBSS, granulocytes were recovered by centrifugation (300  $\times$  g for 7 min) and any remaining erythrocytes were lysed with consecutive additions of 5 ml of ice-cold 0.2% NaCl for 30 s followed by 5 ml of 1.8% NaCl. Following the further addition of 20 ml of HBSS, cells were centrifuged at 300  $\times$  g for 7 min at 4°C. Eosinophils were subsequently isolated by negative selection using CD16<sup>+</sup> MicroBeads as instructed by the manufacturer (Miltenyi Biotec). Briefly, CD16<sup>+</sup> cells (essentially neutrophils) were labeled with CD16<sup>+</sup> MicroBeads and the cell suspension was loaded onto a VarioMACS column. The column was placed in the magnetic field of a MACS Separator and the labeled CD16<sup>+</sup> cells were retained on the column. Unlabeled purified eosinophils were not retained and were washed out and collected. After removal of the column from the magnetic field, the neutrophil fraction was eluted from the column. Eosinophil purity was consistently monitored by Hansel staining and typically ranged above 98%. The levels of activated eosinophils in our preparations ranged between 1% to 3% as estimated by measurement of the activation marker CD69 [11].

### 2.3 2-DE sample preparation

Following CD16<sup>+</sup> MicroBead eosinophil isolation, cells were pelleted at 300  $\times$  g and washed with 30 ml of 1X HBSS. After additional centrifugation at 300  $\times$  g for 7 min cells were solubilized for 2-DE in DeStreak rehydration buffer to a protein concentration of 1  $\mu$ g/ $\mu$ l. If not used immediately for IEF, samples were stored at –80°C. Eosinophils were also subjected to subcellular fractionations using Calbiochem's ProteoExtract<sup>®</sup> Subcellular Proteome Extraction kit according to the manufacturer's provided protocol. Some samples were also

subjected to IEF fractionation using a ZOOM<sup>®</sup> IEF Fractionator (Invitrogen, Carlsbad, CA) following the manufacturer's provided protocol. Ranges of pH collected were 3.0–5.4, 5.4–7.0, and 7.0–10.0. Protein concentrations were established using the RC DC protein assay kit (BioRad). Typically,  $10 \times 10^6$  cells yielded ~500  $\mu\text{g}$  of cell lysate protein.

#### 2.4 2-D gel electrophoresis

Eosinophil protein samples (200  $\mu\text{g}$  for 11 cm and 350  $\mu\text{g}$  for 18 cm IPG strips) were adjusted to 200  $\mu\text{l}$  (11 cm strips) and 350  $\mu\text{l}$  (18 cm strips) with DeStreak rehydration buffer and buffer/ampholyte was added to give a final concentration of 0.5%. The mixtures were microcentrifuged at 2000 rpm for 2 min. IEF was performed with a multi-sample IPGphor (GE Healthcare). Different pH gradient IPG strips were investigated. Paper wicks were placed over each electrode of the ceramic strip holders and 8  $\mu\text{l}$  of Milli-Q H<sub>2</sub>O was added to the wicks just prior to the addition of sample/DeStreak buffer mixtures. Dry IPG strips were added to each sample mixture with the gel side of the strip facing down and the strips were covered with mineral oil. The strip holders were placed in an IPGphor IEF cell and focused at 20°C with the following protocols: for 11 cm IPG strips: 50 V for 11 h (active rehydration), 250 V gradient for 1 h, 500 V gradient for 1 h, 1000 V gradient for 1 h, 8000 V gradient for 2 h, and held at 8000 V for 6 h; for 18 cm IPG strips: 50 V for 11 h, 250 V for 1 h, 500 V for 1 h, 1000 V for 1 h, 8000 V for 2 h, and held at 8000 V for 8 h. IPG strips were then removed and carefully blotted with damp filter paper to remove excess mineral oil. After IEF the strips were equilibrated for 15 min in 4 ml of an equilibration buffer (50 mM Tris-HCL, pH 8.8, containing 6 M urea, 2% SDS, 20% glycerol and 10  $\mu\text{l}/\text{ml}$  TCEP), followed by 15 min of equilibration with 4 ml of the above buffer containing 25 mg iodoacetamide/ml buffer. Strips were then rinsed with 1X Tris-glycine-SDS second dimension electrophoresis running buffer, pH 8.3, and placed in IPG wells of gels with the positive end of the strip toward the left side of the gels. Strips were subsequently overlaid with 0.5% molten agarose. Criterion gels were then placed in a second dimension electrophoresis cell and electrophoresis was conducted using pre-chilled 1X electrophoresis running buffer and 150 V for about 2¼ h or until the bromophenol blue dye reached the gel bottom. The electrophoresis (10°C) protocol for the Protean II gels was as follows: 35 V for 30 min, 50 V for 1 h, 70 V for 1 h, 100 V for 2 h, and 120 V for 12 h or until the dye front reached the bottom of the gel. After the second dimension of electrophoresis the gels were removed from their plates and rinsed with Milli-Q H<sub>2</sub>O prior to staining.

#### 2.5 Fluorescent staining of 2-D gels

Gels were fixed, stained, and destained essentially according to the manufacture's (Invitrogen) recommendations. Briefly, gels intended for Pro-Q Diamond staining were fixed in a solution of 50% methanol and 10% acetic acid in double distilled H<sub>2</sub>O overnight with shaking at RT then washed 3X in double distilled H<sub>2</sub>O, stained in Pro-Q Diamond stain at RT for 90 min, and destained in a solution of 20% acetonitrile, 50 mM sodium acetate (pH 4.0) in double distilled H<sub>2</sub>O. Gels intended for Sypro Ruby staining were fixed in 10% methanol, 7% acetic acid, in double distilled H<sub>2</sub>O for 2 h at RT. Subsequently, the Sypro Ruby stain was applied overnight at RT followed by destaining (10% ethanol) for 1 h. Some gels underwent both staining processes first with Pro-Q Diamond followed by Sypro Ruby.

#### 2.6 Imaging of 2-D gels

Sypro stained gels were imaged at 100  $\mu\text{m}$  resolution with a ProExpress 2-D Proteomic Imaging System (PerkinElmer Life and Analytical Sciences, Waltham, MA) at 460/80 nm excitation and 650/150 nm emission wavelengths. Pro-Q Diamond stained gels were imaged with a Fuji FLA-5100 (Fujifilm USA, Inc., Valhalla, NY) at 532 nm excitation (laser) and 575 nm longpass emission.

## 2.7 2-D gel image analysis

2-DE gel images were analyzed using Progenesis SameSpots software v2.0 (Nonlinear USA, Inc., Durham, NC). This software automatically detects individual protein spots within each image and matches identical protein spots across all images. It also removes noise from measurements of spot volumes using a proprietary algorithm for noise determination and correction. After automatic matching, manual review and adjustments were done to confirm proper spot detection and matching. The intensity of each protein spot was normalized based on the total spot volume of each gel, that is, the spot volume of each spot area was divided by the sum of all spot volumes in the gel. Spots present on less than two gels or with normalized volumes less than 150 were filtered out. Selected spots were robotically picked (Genomic Solutions, Ann Arbor, MI), trypsin digested, and robotically processed (Genomic Solutions) according to the manufacturer's recommendations prior to protein identification by MALDI-MS. Tryptic peptide samples were robotically transferred to MALDI-MS target plates. About 1  $\mu$ l of MALDI matrix solution ( $\alpha$ -cyano-4-hydroxycinnamic acid in 50:50 acetonitrile/H<sub>2</sub>O, 5 mg/ml) was also added robotically to the tryptic samples.

## 2.8 Manual gel sample preparation for MS

When many protein spots were to be picked, we employed the Genomic Solutions robotics instrumentation as described above. However, for those gels with few spots to be picked we used the following manual procedure. Gel samples were cut into 1 mm size pieces and placed into separate 0.5 ml polypropylene tubes. Ammonium bicarbonate buffer (100  $\mu$ l of 50 mM, pH 8.0) was added to each tube and the samples were then incubated at 37°C for 30 min. After incubation, the buffer was removed and 100  $\mu$ l of water was added to each tube. The samples were then incubated again at 37°C for 30 min. After incubation, the water was removed and 100  $\mu$ l of acetonitrile was added to each tube to dehydrate the gel pieces. The samples were vortexed and after 5 min the acetonitrile was removed. Acetonitrile (100  $\mu$ l) was again added to each of the sample tubes, vortexed, and acetonitrile removed after 5 min. The samples were then placed in a speedvac for 45 min to remove any excess solvent. To a 20  $\mu$ g vial of lyophilized trypsin (Promega Corp., Madison, WI) was added 2 ml of 25 mM ammonium bicarbonate (pH 8.0). The trypsin solution was then vortexed and added to each sample tube in an amount required to just cover the dried gel (about 10  $\mu$ l) and the samples were subsequently incubated at 37°C for 6 h. After digestion, the samples were removed from the oven and 1  $\mu$ l of sample solution was spotted directly onto a MALDI target plate and allowed to dry. Subsequently, 1  $\mu$ l of  $\alpha$ -cyano-4-hydroxycinnamic acid matrix solution (50:50 acetonitrile/water at 5 mg/ml) was applied on the sample spot and allowed to air dry.

## 2.9 Mass spectrometry

MALDI TOF/MS was used to analyze tryptic peptide samples and identify proteins. Data were acquired with an Applied Biosystems (Foster City, CA) 4800 MALDI-TOF/TOF Proteomics Analyzer. Applied Biosystems software package included the 4000 Series Explorer (v3.6 RC1) with Oracle Database Schema (v3.19.0), and Data v3.80.0 to acquire both MS and MS/MS spectral data. The instrument was operated in positive ion reflectron mode with a mass range of 850–3000 Da and with the focus mass set at 1700 Da. For MS data, 1000–2000 laser shots were acquired and averaged from each sample spot. Automatic external calibration was performed using a peptide mixture with reference masses 904.468, 1296.685, 1570.677, and 2465.199. Following MALDI-MS analysis, MALDI-MS/MS was performed on several (5–10) of the most abundant ions from each sample spot. A 1 kV positive ion MS/MS method was used to acquire data under post-source decay conditions. The instrument precursor selection window was  $\pm$ 3 Da. For MS/MS data, 2000 laser shots were acquired and averaged from each sample spot. Automatic external calibration was performed using reference fragment masses of 175.120, 480.257, 684.347, 1057.475, and 1441.635 (from precursor mass

1570.700). Applied Biosystems GPS Explorer™ (v3.6) software was used in conjunction with MASCOT (Matrix Science, London, UK) to search the respective protein databases using both MS and MS/MS spectral data for protein identification. Protein match probabilities were determined using expectation values and/or MASCOT protein scores. The expectation value is the number of matches with equal or better scores that are expected to occur by chance alone. The default significance threshold was typically  $p < 0.05$ ; however, for protein identifications herein we used a more stringent threshold of  $10^{-3}$ . The lower the expectation value, the more significant the score. Expectation values were derived from Mascot scores (see [www.matrixscience.com](http://www.matrixscience.com)). MS peak filtering included the following parameters: mass range 800 Da to 4000 Da, minimum S/N filter = 10, mass exclusion list tolerance = 0.5 Da, and mass exclusion list (for some trypsin and keratin-containing compounds) included masses 842.51, 870.45, 1045.56, 1179.60, 1277.71, 1475.79, and 2211.1. For MS/MS peak filtering, the minimum S/N filter was set to 10. For protein identification, the human taxonomy was searched in either the NCBI or SwissProt databases. Other parameters included the following: selecting trypsin; maximum missed cleavages = 1; fixed modifications included carbamidomethyl (C) for 2-D gel analyses only; variable modifications included oxidation (M); precursor tolerance was set at 0.2 Da; MS/MS fragment tolerance was set at 0.3 Da; mass = monoisotopic; and peptide charges were only considered as +1.

### 3 Results

#### 3.1 General characterization of the expression dataset

A representative 2-DE separation of an eosinophil whole cell lysate sample is shown in Fig. 1. The identities of selected non-redundant prominent protein spots are indicated in Table 1. Example of 2-D gels focused over the pH ranges 3–10, 4–7, 5–8, and 6–11 are shown in Fig. 2. In general, eosinophil lysates focused reasonably well in the pH range 3–10. To demonstrate gel to gel reproducibility five gels were selected and the log of normalized spot volumes from gel 1 was plotted pairwise *versus* gels 2 to 5 as shown in Fig. 3 and the Pearson's correlation co-efficient ( $r^2$ ) was calculated. As evident in Fig. 3, the  $r^2$  values indicated that the 2-DE analyses were reasonably reproducible as conducted (mean  $\pm$  SD =  $0.91844 \pm 0.01490$ ). The distribution of proteins identified in the various fractions analyzed (subcellular, IEF, and total lysate) is given in Table 2. Overall, some 3,141 proteins from the 2-DE gels were identified by MALDI-TOF/MS from fractions summarized in Table 2. All of these 3,141 protein spots gave protein IDs with an expectation score of  $< 10^{-3}$ . Of these, 426 proteins identified had unique non-redundant SwissProt identifiers and 231 proteins of the 426 were classified as novel proteins not previously reported to be expressed in eosinophils (Table 1). In general, the fractionation of proteins into the four commercially designated subcellular fractions shown using the ProteoExtract Subcellular Proteome Extraction procedure was quite useful even though some proteins did not distribute authentically; i.e., some proteins distributed correctly according to their known literature localization whereas other proteins did not. For example, many granular proteins (e.g., EPO, ECP, EDN, and MBP) distributed into the cytoskeletal fraction (F4) and most of the actin was in the nuclear fraction (F3). However, in general, the subcellular fractionation method principally proved valuable in reducing protein complexity and increasing low abundance proteins. Fig. 4 is a Western blot analysis that shows the distribution of eight randomly selected proteins into the four subcellular fractions (F1 to F4) demonstrating in part the effectiveness of the differential fractionation method.

Actin was the most prominent protein expressed in eosinophils. Because of this fact, we chose to comparatively evaluate actin levels in other leukocytes. Fig. 5 shows the comparative distribution of actin and an actin proteolytic cleavage fragment by Western blot analysis of monocyte, neutrophil, and eosinophil cell lysates.

### 3.2 Ingenuity Pathway Analysis software application

Ingenuity software was applied to the analysis of the eosinophil expression dataset to probe the relevant biological functions of the identified proteins in the dataset (Table 1). Some functions and diseases relevant to the dataset are shown in Fig. 6. Fig. 7 shows selected groups of proteins that highlight in more detail the proportion of the identified proteins whose function or impact are particularly relevant to eosinophil biological activity; namely, immunological disease, inflammatory disease, immune response, immune and lymphatic system development and function, and respiratory disease. Fig. 8 gives a histogram of the top canonical pathways associated with the dataset. A small p-value indicated a strong association between the dataset and the respective pathway. Proteins found in selected eosinophil disease functional and canonical pathway subsets (Figs. 6 and 8) are listed in supplemental Tables S1 and S2 (see [www.proteomics-journal.com](http://www.proteomics-journal.com)).

## 4 Discussion

We have identified 3,141 proteins which had Mascot expectation scores of  $10^{-3}$  or less. Of these, 426 proteins were unique and non-redundant as identified using the SwissProt protein database. We did not attempt to distinguish differences between males and females nor did we address the extent of observed polymorphic variations between individuals since large numbers of donors would be required. However, further studies are planned to deal with these important issues. Significantly, of the 426 non-redundant proteins 231 were novel proteins not previously reported to occur in eosinophils. Since only 8% of all proteins excised and analyzed from 2-D gels were among the unique, non-redundant dataset (426 proteins), the question arises as to the occurrence and nature of the redundant protein dataset (2715 proteins).

There are many explanations for protein redundancy including phosphorylation. We undertook a preliminary assessment of the eosinophil phosphoproteome using Pro-Q Diamond staining in order to evaluate the contribution of phosphorylation to redundancy (results not shown). The characterization of the eosinophil phosphoproteome by 2-DE will be separately reported. We found that many eosinophil proteins were phosphorylated; phosphorylation can be variable at a given site and may be variable as to the number of sites modified all of which contribute to redundancy. In addition, as shown in Fig. 1, 2-D gel analysis indicated a number of horizontal protein spots, identified as the same protein by MS, with the same Mr but having different pIs, indicating polymorphism and/or posttranslational modification. In addition to phosphorylation, a number of modifications can account for such variations; as for example, acetylation, sialylation, sulfation, and methylation. Furthermore, since many proteins have attached carbohydrate moieties, these can give rise to significant pI and/or Mr variations. Finally, proteolytic processing/modifications must be considered among the relevant causes of protein redundancy. Clearly, the above examples are not an exhaustive list of factors leading to protein redundancies. The observed high protein redundancy likely reflected the dynamic character of the eosinophil and underscores the fact that posttranslational modifications may be the result of various regulatory and signaling events.

This proteomic dataset is the largest comprehensive proteomic dataset of proteins expressed in normal peripheral blood eosinophils reported to date. There have been two reports of comparative proteomic studies. Waschnagg *et al.* [12] very recently evaluated protein expression differences induced by Birch pollen allergy and identified 97 unique non-redundant eosinophil proteins of which 90 occur in our list of 426 (Table 1) which is an excellent agreement. However, a comparative proteomic study of healthy *versus* atopic dermatitis patients identified 51 differentially expressed proteins of which only three are included in Table 1 [13].

In this study we have made some attempt at characterizing the less abundant proteins using ZOOM<sup>®</sup> pre-fractionation IEF and subcellular fractionation methods. Protein distribution into various fractions using a commercial subcellular fractionation method allowed for the reduction of protein complexity and increased the number of less abundant proteins observed. We found that this fractionation method performed better in reducing protein losses than many other subcellular fractionation methods that can incur appreciable protein loss. Furthermore, the differential solubilization method was amenable to small sample size, gave high protein recoveries, had relatively high throughput, and processing time was fairly short minimizing protein alterations. However, this method is not sufficiently adequate to predict protein localization to specific subcellular compartments.

Characterization of the dataset (Table 1) using Ingenuity Pathway Analysis revealed a number of interesting features. Especially worthy of note was that 312 of the 434 (72%) identified non-redundant proteins could be subdivided into categories (Fig. 6) which were related to known eosinophil biological activities directly; e.g., eosinophilia, cell movement, chemotaxis and activation, or indirectly; e.g., autoimmune diseases. We were able to detect and positively identify many proteins that were relevant to eosinophil functions involving survival and activation. Recent studies strongly suggest that tissue eosinophilia is more dependent on increased survival in peripheral tissues than increased *de novo* generation in the bone marrow followed by blood to tissue translocation [14]. Analysis of eosinophil turnover *in vivo* revealed their active recruitment to the peritoneal cavity and their prolonged survival there [14]. In this regard our Ingenuity Pathway analysis showed a considerable number of proteins (~125) involved in cell death and survival (Fig. 6). Most of these proteins have previously not been correlated with eosinophil survival processes. However, some of these proteins were shown to play roles in other aspects of eosinophil biology. These observations emphasized the need for more studies to investigate the pro- and anti-apoptotic proteins that regulate eosinophil survival in end organs to induce or prevent apoptosis in cells depending on whether the need is to protect against helminth parasites or ameliorate eosinophil-associated diseases.

Eosinophils are secretory cells that contain large amounts of granules occupying about one-fifth of the cytoplasm [1]. Four major populations of granules have been identified; namely, primary, secondary, small granules, and as well lipid bodies [1]. Our 2-DE studies identified four of the major proteins found in the secondary granules that included, ECP, EDN, EPO, and MBP as well as galectin-10 found in the primary granules. Numerous other proteins have also been reported to occur in the granules [1]. ECP is a secretory ribonuclease associated with host defense against nonphagocytosable pathogens, such as helminthic parasites. It also has antibacterial activity which is not shared by EDN, another closely-related neurotoxic eosinophil ribonuclease. The mechanism of action of ECP is thought to involve pore formation in target membranes which is apparently not dependent on its RNase activity [15]. On the other hand, EDN which shares 70% homology with ECP has been implicated in antiviral activity against respiratory infections mainly due to its ribonuclease activity [16]. EPO is an eosinophil haloperoxidase that catalyzes the peroxidative oxidation of halides present in the plasma as well as hydrogen peroxide generated by dismutation of superoxide produced during respiratory burst. This reaction leads to the formation of bactericidal hypohalous acids [17]. MBP was traditionally associated with toxicity against helminthic worms and is at least partly responsible for tissue damage in bronchial mucosa in asthma. The mechanism of its action is believed to be increased membrane permeability through surface charge interactions leading to perturbation of the cell-surface lipid bi-layer. These granule proteins are actively released from activated eosinophils and little if any active transcription occurs in mature eosinophils. The role of eosinophils in the pathophysiology of bacterial and viral infections is still not well elucidated.



The second most abundant and notable protein observed by 2-D gel analysis of eosinophil cell lysates was galectin-10 (Table 1, Fig. 1; ID 329) which occurs mainly in the primary granules of eosinophils and for many years was referred to as lysophospholipase or Charcot-Layden crystal protein. However, new evidence gives strong indication that it belongs to the galectin superfamily of proteins and was designated as galectin-10 by Ackerman *et al.* [18, 19]. Previously galectin-10 was thought to occur only in eosinophils and basophils but recent work has also identified it in human CD4<sup>+</sup>CD25<sup>+</sup> regulatory T cells (CD25<sup>+</sup> Treg cells) where it is thought to function in maintaining immunological self-tolerance by suppressing autoaggressive T-cells [20]. Eosinophilic galectin-10 also appears to have lectin-like properties and can bind mannose (in the crystal) [18]. Further investigations are required to elucidate the biological function of this interesting protein. Gel analysis results from both 1-D and 2-D gels, including Western blot analysis using anti-galectin-10, showed that galectin-10 distributed in multiple gel locations. Repeated gel analysis by 1D SDS-PAGE and Western blotting of eosinophil cell lysates gave three bands of molecular weights ~ 17 KDa, ~ 25 KDa, and ~ 75 KDa. Galectin-10 has been reported to be unique in having a propensity to aggregate even in dissociating conditions [21]. Gel analysis by 2-DE was also anomalous with spots at ~ 17 KDa and ~ 25 KDa and pronounced vertical streaking likely due to precipitation at its *pI* in the first dimension of 2-DE (Fig. 1). Some dimer formation was also noted (Fig. 1). Western blot 2-DE analysis of galectin-10 also showed multiple horizontal spots at ~ 17 KDa indicating polymorphism and/or posttranslational modifications. N-terminal acetylation and isoforms for galectin-10 were also identified by 2-DE of CD25<sup>+</sup> Treg-cell lysates and human eosinophils [20]. A separate study will be required to fully characterize the various isoforms associated with galectin-10.

The 2-D gels showed that eosinophils have especially high amounts of actin (Fig. 1, Table 1; ID 311) which contributed to the relatively lower abundance of other proteins in the cell lysate samples. Actin cytoskeletal structures and associated proteins likely play important roles in eosinophil functions; such as, signaling (Fig. 8), cell motility, degranulation, phagocytosis, and activation [22–24]. Some of the actin was proteolytically processed to smaller Mr forms (Figs. 1 and 5; Table 1; ID 275) and some actin was also phosphorylated (Pro-Q Diamond staining not shown). Actin phosphorylation in other cells was previously reported [25, 26] and plays an important role in actin polymerization [27, 28]. Protein MS identification did not distinguish between  $\beta$ - or  $\alpha$ -actin since  $\beta$ - and  $\alpha$ -actin have virtually identical primary structures. Although nonmuscle actin and actin-associated proteins are reported to occur in the nucleus of cells [29], our previous studies using FITC-phalloidin, anti- $\alpha$ -fodrin [24], and anti-actin (results not shown) did not indicate the occurrence of nuclear actin in eosinophils. However, these results could not rule out the occurrence of very low levels of nuclear actin that could not be detected under the experimental conditions employed or that the actin Ab was not reactive to nuclear actin due to some unique complex formation. Actin levels in eosinophils and monocytes were relatively high when compared with neutrophils with considerably more proteolytic processing occurring in monocytes (Fig. 5). This was also confirmed by 2-DE of cell lysates (results not shown). The observed actin fragment represented the N-terminal domain of actin, since the anti-actin antibody used was raised against an N-terminal fragment (actin 1–19). Numerous actin complex-associated proteins were identified; for example, actin-related protein 2/3 complex, gelsolin, vimentin, Rho GDP-dissociation inhibitor, transgelin, moesin, coactosin-like protein, tubulin, cofilin, L-plastin, calreticulin, myosin, F-actin capping proteins cap Z alpha-1 and beta, and macrophage protein G,  $\alpha$ -actinin, profilin, dynactin, coronin, nesprin, kinesin, tropomodulin, talin, and spectrin. The facile identification of these proteins was undoubtedly related to the high level expression of cytoplasmic actin in eosinophils. The high actin level and abundant associated proteins underscore the importance of the cytoskeleton in the biological activity of eosinophils especially motility and activation

An important advantage of proteomic analysis by 2-DE is the visualization and potential identification of polymorphisms and/or posttranslational modifications. Fig. 1 shows a number of proteins that are likely to be posttranslationally modified as evidenced by repeated horizontal protein spots from the same protein identified by MS; for example, Fig. 1, Table 1; ID's 31, 36, 45, 48, 49, 50, 53, 59, 61, 66, 107, 135, 167, 182, 193, 216, 257, 283, 304 and 329. Some of these proteins have not been previously reported to be posttranslationally modified; as for example, Table 1: 31, 59, 107, 135, and 257. We expect that the herein described protein expression results represent the largest.

In summary, the herein described protein expression results represent the largest comprehensive reporting of the human eosinophil proteome. The identification of proteins in any proteome study is somewhat asymptotic and probably not 100% achievable by current technologies. This proteome map will be especially valuable as a baseline to compare with eosinophils from disease and pharmacologically treated states.

## Supplementary Material

Refer to Web version on PubMed Central for supplementary material.

## Abbreviations

<b>HBSS</b>	Hank's balanced saline solution
<b>TCEP</b>	tri-(2-carboxyethyl) phosphine
<b>IPG</b>	immobilized pH gradient
<b>RT</b>	room temperature
<b>GM-CSF</b>	granulocyte-macrophage colony-stimulating factor
<b>RANTES</b>	regulated upon activation, normal T cell expressed and secreted
<b>ID</b>	identification
<b>EOS</b>	eosinophil
<b>IPA</b>	Ingenuity Pathway Analysis
<b>EPO</b>	eosinophil peroxidase
<b>MBP</b>	major basic protein
<b>ECP</b>	eosinophil cationic protein
<b>EDN</b>	eosinophil-derived neurotoxin
<b>CLC</b>	Charcot-Leyden crystal protein
<b>IL</b>	interleukin

## Acknowledgments

### Funding information

This study was supported by the National Institutes of Health, National Heart, Lung and Blood Institute's Proteomics Initiative NO1-HV-28184 (to A. K.), the National Institutes of Health grants 1-R24 CA88317 (to A.K.), 1-P30 ES06676 (to C. Elferink) and 1-P01AI062885 (to A. Brasier).

## References

1. Giembycz MA, Lindsay MA. Pharmacology of the eosinophil. *Pharmacol. Rev* 1999;51:213–339. [PubMed: 10353986]
2. Rothenberg ME, Hogan SP. The eosinophil. *Annu. Rev. Immunol* 2006;24:147–174. [PubMed: 16551246]
3. Ganley-Leal LM, Mwinzi PN, Cetre-Sossah CB, Andove J, et al. Correlation between eosinophils and protection against reinfection with *Schistosoma mansoni* and the effect of human immunodeficiency virus type 1 coinfection in humans. *Infect. Immun* 2006;74:2169–2176. [PubMed: 16552047]
4. Melo RCN, Spencer LA, Dvorak AM, Weller PF. Mechanisms of eosinophil secretion: large vesiculotubular carriers mediate transport and release of granule-derived cytokines and other proteins. *J. Leukoc. Biol* 2008;83:229–236. [PubMed: 17875811]
5. Pazdrak K, Young TW, Stafford S, Olszewska-Pazdrak B, Straub C, et al. Cross-Talk between ICAM-1 and granulocyte-macrophage colony-stimulating factor receptor signaling modulates eosinophil survival and activation. *J. Immunol* 2008;180:4182–4190. [PubMed: 18322230]
6. Matsumoto K, Appiah-Pippim J, Schleimer RP, Bickel CA, et al. CD44 and CD69 represent different types of cell-surface activation markers for human eosinophils. *Am. J. Respir. Cell Mol. Biol* 1998;18:860–866. [PubMed: 9618391]
7. Wardlaw A. Eosinophil density: what does it mean? *Clin. Exper. Allergy* 1995;25:1145–1149. [PubMed: 8821292]
8. Gruart V, Balloul JM, Prin L, Tomassini M. Variations in protein expression related to human eosinophil heterogeneity. *J. Immunol* 1989;142:4416–4421. [PubMed: 2723435]
9. Fukuda T, Gleich GJ. Heterogeneity of human eosinophils. *J. Allergy Clin. Immunol* 1989;83:369–373. [PubMed: 2645342]
10. Pleis JR, Lethbridge-Cejku M. *Summary Health Statistics for U.S. Adults: National Health Interview Survey*, Vital Health Stat 2007;10(235)
11. Matsumoto K, Appiah-Pippim J, Schleimer RP, Bickel CA, et al. CD44 and CD69 represent different types of cell-surface activation markers for human eosinophils. *Am. J. Respir. Cell Mol. Biol* 1998;18:860–866. [PubMed: 9618391]
12. Waschnagg C, Forsberg J, Engström Å, Odreman F, Venge P, Garcia R. The human eosinophil proteome. Changes induced by Birch pollen allergy. *J. Proteome Res.* 2009 DOI: 10.1021/pr800984e.
13. Yoon SW, Kim TY, Sung MH, Kim CJ, Poo H. Comparative proteomic analysis of peripheral blood eosinophils from healthy donors and atopic dermatitis patients with eosinophilia. *Proteomics* 2005;5:1987–1995. [PubMed: 15832365]
14. Ohnmacht CPullner AVan Rooijen NVoehringer DAnalysis of eosinophil turnover *in vivo* reveals their active recruitment to and prolonged survival in the peritoneal cavity. *J. Immunol* 2007;179:4766–4774 [PubMed: 17878375]
15. Domachowske JB, Dyer KD, Adams AG, Leto TL, Rosenberg HF. Eosinophil cationic protein/RNase 3 is another RNase A-family ribonuclease with direct antiviral activity. *Nucleic Acids Res* 1998;26:3358–3363. [PubMed: 9649619]
16. Rosenberg HF. Eosinophil-derived neurotoxin/RNase 2; connecting the past, the present and the future. *Curr. Pharm. Biotechnol* 2008;9:135–140. [PubMed: 18673278]
17. Jong EC, Henderson WR, Klebanoff SJ. Bactericidal activity of eosinophil peroxidase. *J. Immunol* 1980;124:1378–1382. [PubMed: 6987309]
18. Ackerman SJ, Liu L, Kwatia MA, Savage MP, et al. Charcot-Leyden crystal protein (galectin-10) is not a dual function galectin with lysophospholipase activity but binds a lysophospholipase inhibitor in a novel structural fashion. *J. Biol. Chem* 2002;277:14859–14868. [PubMed: 11834744]
19. Ackerman SJ, Corrette SE, Rosenberg HF, Bennett JC, et al. Molecular cloning and characterization of human eosinophil Charcot-Leyden crystal protein (lysophospholipase). *J. Immunol* 1993;150:456–468. [PubMed: 8419478]
20. Kubach J, Lutter P, Bopp T, Stoll S, et al. Human CD4<sup>+</sup>CD25<sup>+</sup> regulatory T cells: proteome analysis identifies galectin-10 as a novel marker essential for their energy and suppressive function. *Blood* 2007;110:1550–1558. [PubMed: 17502455]

21. Ackerman SJ, Loegering DA, Gleich GJ. The human eosinophil Charcot-Leyden crystal protein: biochemical characteristics and measurement by radioimmunoassay. *J. Immunol* 1980;125:2118–2126. [PubMed: 7430621]
22. Boehme SA, Sullivan SK, Crowe PD, Santos M, et al. Activation of mitogen-activated protein kinase regulates eotaxin-induced eosinophil migration. *J. Immunol* 1999;163:1611–1618. [PubMed: 10415066]
23. Suzuki M, Kato M, Hanaka H, Izumi T, et al. Actin assembly is a crucial factor for superoxide anion generation from adherent human eosinophils. *J. Allergy Clin. Immunol* 2003;112:126–133. [PubMed: 12847489]
24. Starosta V, Pazdrak K, Boldogh I, Svider T, Kurosky A. Lipoxin A<sub>4</sub> counterregulates GM-CSF signaling in eosinophilic granulocytes. *J. Immunol* 2008;181:8688–8699. [PubMed: 19050289]
25. Rush J, Moritz A, Lee KA, Guo A, et al. Immunoaffinity profiling of tyrosine phosphorylation in cancer cells. *Nat. Biotech* 2004;23:94–101.
26. Zahedi RP, Lewandrowski U, Wiesner J, Wortelkamp S, et al. Phosphoproteome of resting human platelets. *J. Proteome Res* 2008;7:526–534. [PubMed: 18088087]
27. Liu X, Shu S, Hong MSS, Levine RL, Korn ED. Phosphorylation of actin Tyr-53 inhibits filament nucleation and elongation and stabilizes filaments. *Proc. Natl. Acad. Sci. USA* 2006;103:13694–13699. [PubMed: 16945900]
28. Wang S, Zheng Y, Yu Y, Xia L, et al. Phosphorylation of  $\beta$ -actin by protein kinase C-delta in camptothecin analog-induced leukemic cell apoptosis. *Acta Pharmacol. Sinica* 2008;29:135–142.
29. Pederson T, Aebi U. Actin in the nucleus: what form and what for? *J. Struct. Biol* 2003;140:3–9. [PubMed: 12490148]

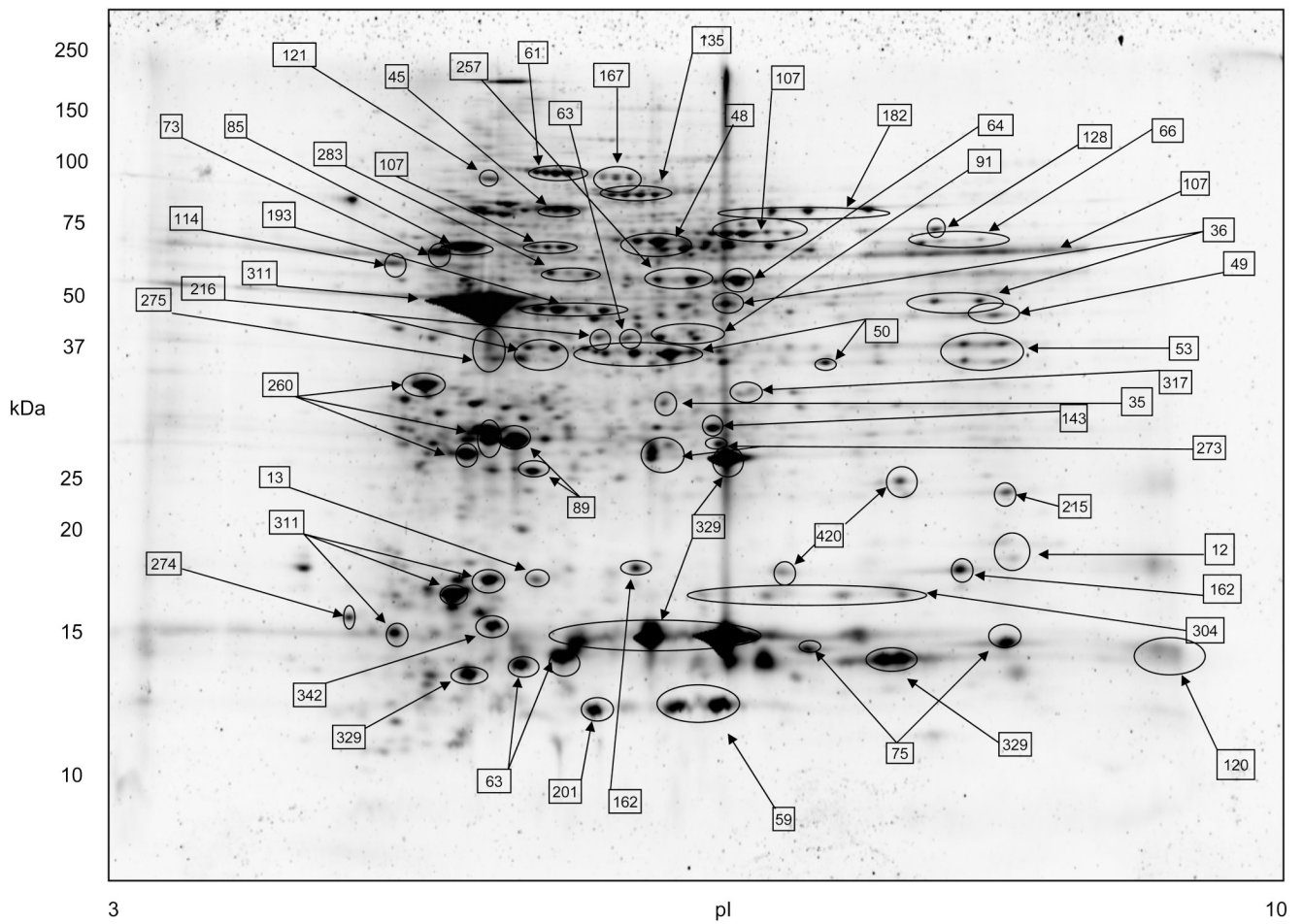


**Figure 1.**

The proteome map of human peripheral blood eosinophils. Isoelectric focusing was conducted in the pH range 3 to 10 in the first dimension. Major protein spots indicated by arrows are identified in Table 1. Protein vertical streak was due to galectin-10 insolubility (see Discussion). 200  $\mu$ g of total eosinophil cell lysate was loaded to the gel.

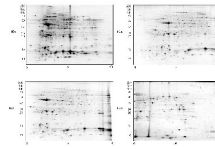


**Figure 2.** Comparison of eosinophil proteome maps focused at four different pH ranges: 3–10; 4–7; 5–8; and 6–11. Each gel was loaded with 200  $\mu$ g of total eosinophil cell lysate.

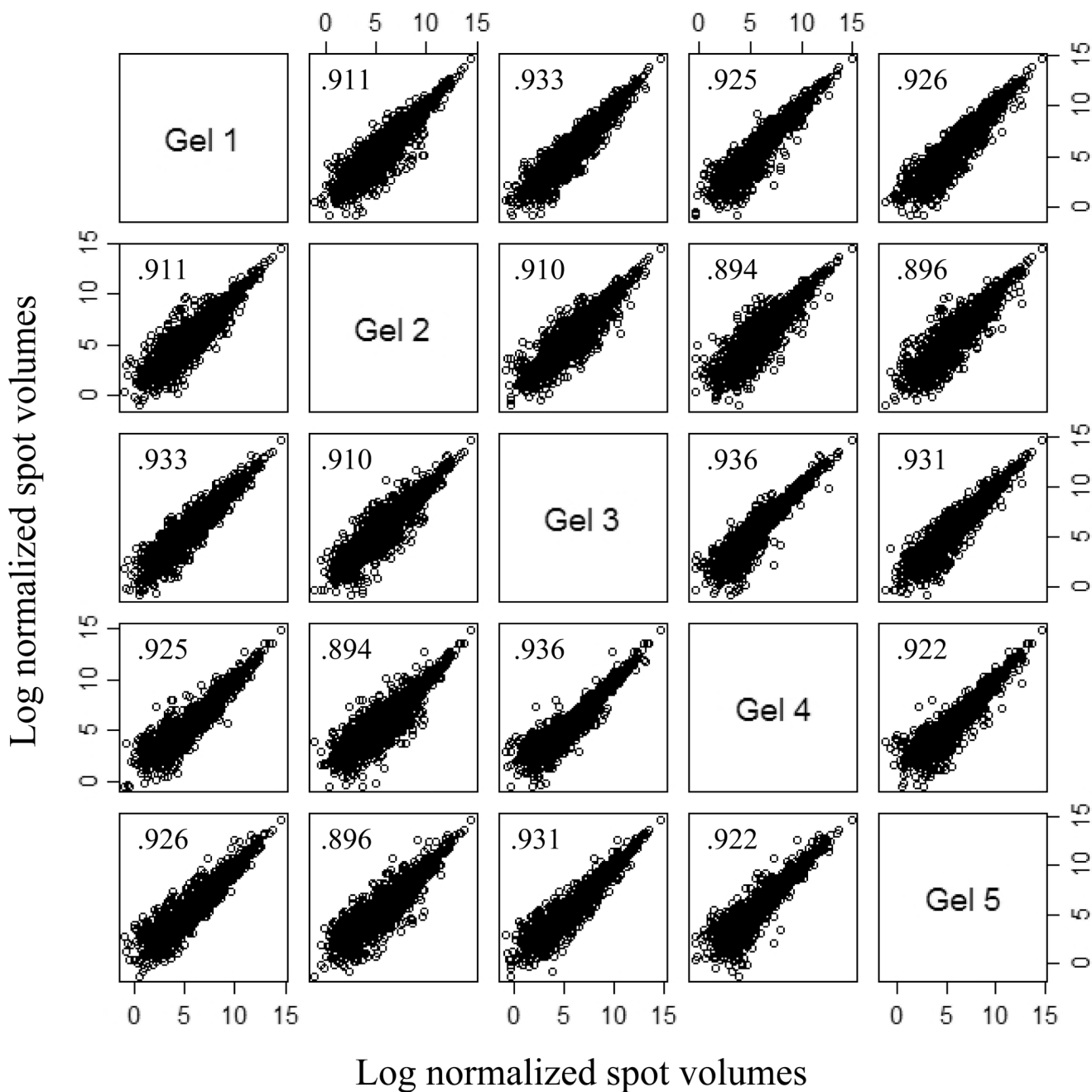


**Figure 3.** Gel-to-gel correlation of five replicate gels showing 2-DE reproducibility. Log normalized spot volumes for gel 1 were plotted pairwise versus gels 2 to 5 and the Pearson's correlation coefficient shown in squares was calculated. Gels (11 cm) were focused over the pH range 3–10 and were stained with Sypro Ruby. Gel image analysis utilized Nonlinear SameSpots software.

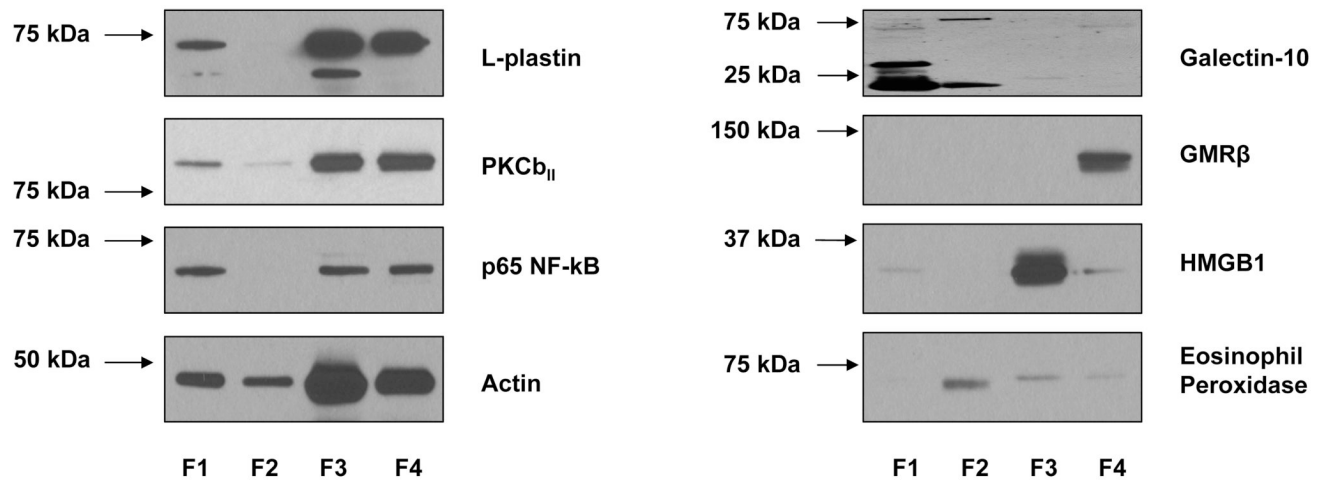


**Figure 4.**

Western blot analysis of eight randomly selected eosinophil proteins to demonstrate their distribution by differential solubility using a commercial kit (Calbiochem's ProteoExtract<sup>®</sup> Subcellular Proteome Extraction kit). The kit employed four solubility fractions F1 to F4 as shown (see also Table 2). 50  $\mu$ g of cell lysates were applied to each lane.



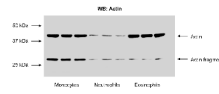


**Figure 5.** Western blot analysis comparing actin levels in monocytes, neutrophils, and eosinophils in triplicate. 50  $\mu$ g of cell lysate protein was loaded in each lane. Actin fragment was an N-terminal product as a result of proteolysis (see Discussion).

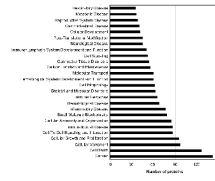


**Figure 6.** Ingenuity Pathway Analysis showing the distribution of identified eosinophil proteins from Table 1 into disease and functional categories.

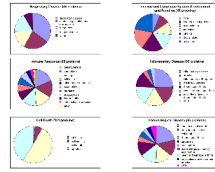


**Figure 7.** Subclassification of eosinophilic proteins from Table 1 and Fig. 6 shows a distribution of eosinophilic proteins into diseases and functional categories highly consistent with what is general appreciated regarding eosinophilic biological activity.

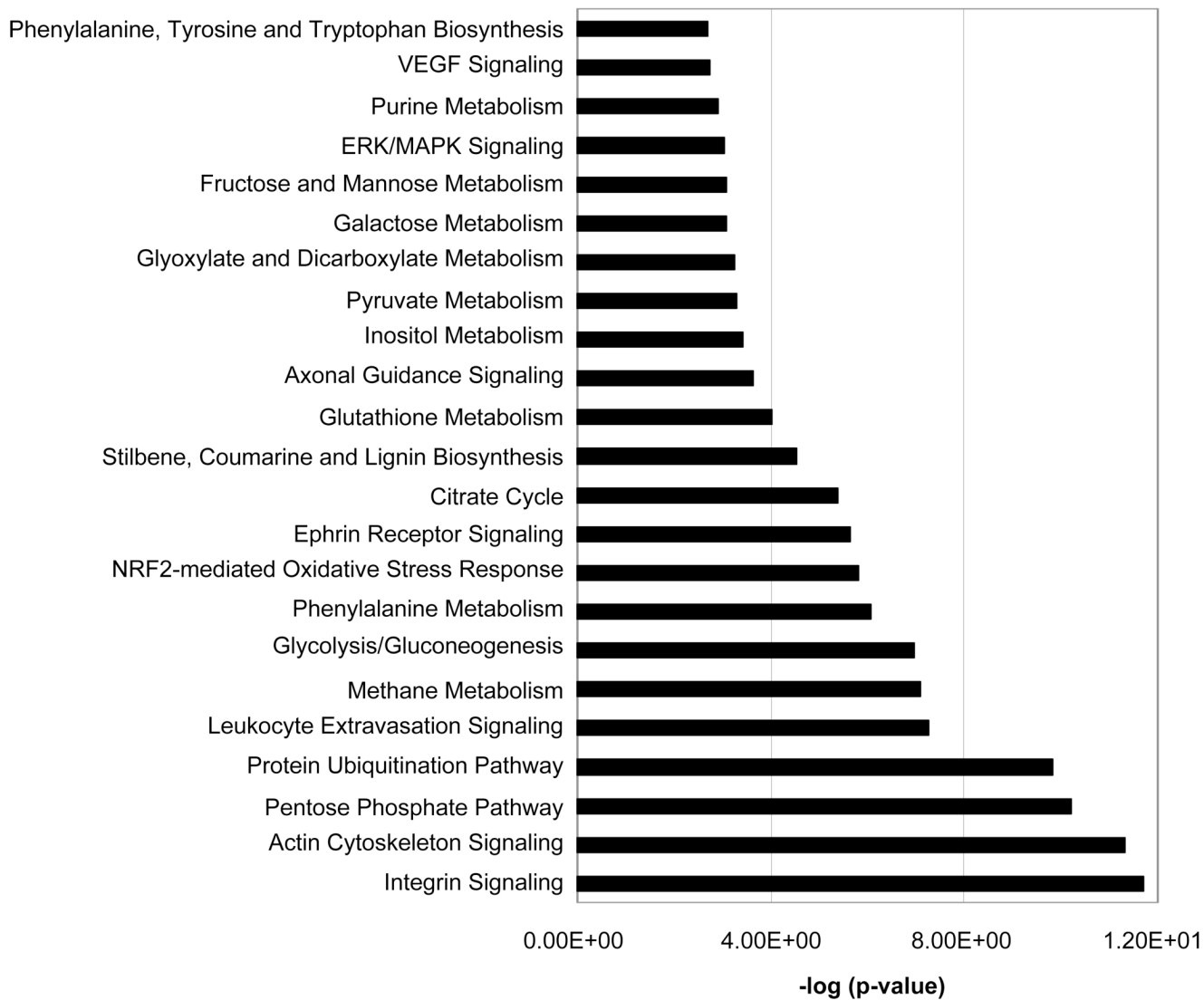


**Figure 8.** Ingenuity Pathway Analysis showing the distribution of identified eosinophil proteins (Table 1) into canonical pathways showing a strong emphasis on signaling pathways consistent with the dynamic nature of the eosinophil.

Table 1

List of identified proteins with significant SwissProt IDs

ID No.	Protein Name	Swiss Prot Access. no. <sup>a</sup>	Theoret./observ. pI <sup>b</sup>	Theoret./Observ. Mr <sup>c</sup> (kDa)	Pept. Match h (n)	Seq. cov. <sup>d</sup> (%)	Mascot expect. score <sup>e</sup>	Sub. cell. Fract. No. <sup>f</sup>
1	Actin capping protein	A4D0V4	ND <sup>g</sup>	ND	ND	ND	8.70E-19	6
2	AH receptor-interacting protein	O00170	6.09/6.44	38.10/64.84	11	39	1.50E-06	2
3	Hunc18b2	O00184					4.40E-08	6
4	26S proteasome non-ATPase regulatory subunit 11	O00231	6.09/6.39	47.72/85.60	4	10	4.90E-03	3
5	Chloride intracellular channel	O00299	5.09/5.68	27.25/53.71	5	19	6.90E-04	5
6	26S proteasome non-ATPase regulatory subunit 14	O00487	6.06/6.34	34.73/68.86	8	35	2.70E-04	3
7	Lysosomal alpha-mannosidase precursor	O00754	6.84/5.95	114.36/97.37	13	15	2.70E-28	4
8	Proteasome subunit alpha type 7	O14818	8.60/8.50	28.04/58.91	11	50	2.90E-16	5
9	Ras-related protein Rab-7L1	O14966	6.73/6.66	23.43/40.18	9	52	2.20E-03	3
10	Actin-related protein 2/3 complex subunit 1B	O15143	8.69	41.72	6	22	9.98E-05	6
11	Actin-related protein 2/3 complex subunit 2	O15144	6.84/6.90	34.43/57.04	22	63	5.80E-48	3
12	Actin-related protein 2/3 complex subunit 3	O15145	8.82/8.49	20.76/28.61	7	35	1.90E-06	1
13	Actin-related protein 2/3 complex subunit 5	O15511	5.47/5.87	16.37/27.15	7	56	1.30E-17	3
14	Thioredoxin-like protein 1	O43396	4.84/5.50	32.63/68.45	11	50	1.30E-11	3
15	Mitotic checkpoint protein	O43684	6.36/6.68	37.59/70.09	15	46	2.90E-19	2
16	Alpha-actinin-4	O43707	5.27/5.72	105.24/184.80	35	46	1.20E-29	3
17	Keratin, type II cuticular Hb6	O43790	5.56/6.24	55.12/215.17	22	48	2.70E-16	1
18	Glia maturation factor gamma	O60234	5.18/5.48	16.96/28.19	11	58	1.50E-23	1
19	Sorting nexin-3	O60493	8.73/8.41	18.81/24.55	9	51	1.10E-04	5
20	Docking protein 2	O60496	6.58/5.93	45.75/84.31	16	32	2.10E-18	2
21	Protein diaphanous homolog 1	O60610	ND	ND	ND	ND	4.80E-03	6
22	Mannose-6-phosphate receptor-binding protein 1	O60664	ND	ND	ND	ND	6.10E-11	6
23	Histone H2B type 1-K	O60814	10.32/9.09	13.75/27.17	7	53	2.70E-15	3
24	WD repeat protein 1	O75083	6.18/6.60	66.84/126.16	16	40	4.30E-18	3
25	Copine-3	O75131	5.60/5.98	60.95/112.67	14	26	1.20E-13	1

ID No.	Protein Name	Swiss Prot Access. no. <sup>a</sup>	Theoret./observ. pI <sup>b</sup>	Theoret./Observ. Mr <sup>c</sup> (kDa)	Pept. Matic h (n)	Seq. cov. <sup>d</sup> (%)	Mascot expect. score <sup>e</sup>	Sub. cell. Fract. No. <sup>f</sup>
26	SH3 domain-binding glutamic acid-rich-like protein	O75368	5.22/5.79	12.76/20.10	3	35	3.20E-04	1
27	Citrate synthase, mitochondrial precursor	O75390	8.45/8.20	51.91/71.91	12	20	2.30E-34	4
28	Protein CREG1 precursor	O75629	7.05/6.61	24.17/39.66	3	15	1.90E-03	4
29	Protein XRP2	O75695	5.00/5.41	40.47/73.37	12	30	3.60E-06	3
30	6-Phosphogluconolactonase	O95336	5.70/6.09	27.81/52.24	14	37	1.80E-35	1
31	Ras-related protein Rab-3D	O95716	4.76/5.01	24.48/46.39	14	49	5.80E-13	3
32	L-Lactate dehydrogenase A chain	P00338	8.44/6.11	36.95/106.74	14	33	2.10E-17	5
33	Glutamate dehydrogenase 1, mitochondrial precursor	P00367	7.66/7.01	61.70/95.99	14	29	2.90E-11	3
34	Glutathione reductase, mitochondrial precursor	P00390	8.74	56.79	14	34	1.26E-29	6
35	Purine nucleoside phosphorylase	P00491	6.45/6.57	32.33/58.66	14	75	5.80E-45	5
37	Carbonic anhydrase 1	P00915	6.59/8.34	28.91/71.39	14	58	3.40E-28	4
38	Carbonic anhydrase 2	P00918	6.87/7.13	29.28/58.26	14	40	2.70E-12	1
39	Alpha-1-antitrypsin precursor	P01009	5.37/5.40	46.88/89.30	14	21	1.20E-07	1
40	Alpha-1-antichymotrypsin precursor	P01011	5.33/4.77	47.49/111.08	14	30	3.60E-09	3
41	Hemoglobin subunit delta	P02042	7.85/8.67	16.16/16.71	14	95	8.50E-23	4
42	Spectrin alpha chain, erythrocyte	P02549	4.96/5.37	280.88/219.26	14	15	1.30E-04	1
43	Fibrinogen beta chain precursor	P02675	8.54	56.58	14	43	2.51E-14	6
44	Transferrin precursor	P02766	5.52/6.13	15.99/25.35	14	63	5.80E-13	3
45	Serum albumin precursor	P02768	5.92/6.30	71.32/34.20	14	34	9.20E-28	2
46	Lactoferrin precursor	P02788	8.50/7.16	80.01/167.43	14	61	1.50E-89	3
47	Ferritin light chain	P02792	5.51/5.97	20.06/93.00	14	46	1.30E-30	3
48	Catalase	P04040	6.95/6.73	59.82/118.28	14	29	2.10E-64	6
49	Fructose-bisphosphate aldolase A	P04075	8.39/8.45	39.85/73.95	14	36	1.10E-12	5
50	Annexin A1	P04083	6.64/6.39	38.92/66.84	14	70	2.10E-92	1
51	Superoxide dismutase [Mn], mitochondrial precursor	P04179	8.35/6.15	24.88/42.73	14	16	1.90E-03	4
52	Keratin, type II cytoskeletal I	P04264	8.16/6.09	66.02/53.75	14	32	5.40E-49	5
53	Glyceraldehyde-3-phosphate dehydrogenase	P04406	8.58/8.52	36.21/57.25	14	57	8.50E-14	5

ID No.	Protein Name	Swiss Prot Access. no. <sup>a</sup>	Theoret./observ. p <sup>b</sup>	Theoret./Observ. Mr <sup>c</sup> (kDa)	Pept. Match (n)	Seq. cov. <sup>d</sup> (%)	Mascot expect. score <sup>e</sup>	Sub. cell. Fract. No. <sup>f</sup>
54	Calpain small subunit 1	P04632	5.05/5.29	28.47/51.56	14	30	7.30E-09	3
55	Cytochrome b-245 heavy chain	P04839	8.90/7.20	66.21/26.85	14	17	1.30E-05	4
56	Guanine nucleotide-binding protein G(i), alpha-2 subunit	P04899	ND	ND	ND	ND	2.20E-45	6
57	Aldehyde dehydrogenase, mitochondrial precursor	P05091	6.63/7.06	56.86/62.30	15	30	2.30E-35	4
58	Integrin beta-2 precursor	P05107	6.69/6.22	87.98/88.07	29	39	2.70E-23	4
59	Protein S100-A8	P05109	6.51/6.39	10.85/45.31	10	82	1.80E-20	5
60	Myeloperoxidase precursor	P05164	9.19/9.75	84.78/90.76	23	31	3.60E-24	5
61	Gelsolin precursor	P06396	5.90/6.32	86.04/131.40	21	29	1.50E-52	5
62	ATP synthase subunit beta, mitochondrial precursor	P06576	5.26/5.40	56.52/95.54	20	52	1.20E-59	3
63	Protein S100-A9	P06702	5.71/8.70	13.29/282.65	6	50	5.80E-22	5
64	Alpha-enolase	P06733	6.99/5.82	47.48/145.56	18	44	8.50E-15	5
65	Glycogen phosphorylase, liver form	P06737	6.71/6.84	97.49/184.17	32	41	6.80E-50	5
66	Glucose-6-phosphate isomerase	P06744	8.43/8.23	63.34/101.91	25	51	2.10E-32	5
67	Tropomyosin alpha-3 chain	P06753	ND	ND	ND	ND	3.00E-33	6
68	L-Lactate dehydrogenase B chain	P07195	5.72/6.02	36.90/62.40	14	47	6.80E-24	1
69	Glutathione peroxidase 1	P07203	6.15/5.97	22.27/36.59	10	69	7.30E-11	2
70	Protein disulfide-isomerase precursor	P07237	4.76/5.17	57.48/107.61	25	57	5.80E-79	3
71	Cathepsin D precursor	P07339	6.10/5.98	45.04/52.24	14	40	2.90E-15	1
72	Annexin A2	P07355	7.57/7.62	38.81/72.03	19	49	2.70E-26	1
73	Tubulin beta-2 chain	P07437	4.78/5.29	50.10/97.65	22	55	8.50E-28	3
74	Beta-hexosaminidase beta chain precursor	P07686	6.29	63.53	11	19	9.98E-05	6
75	Profilin-1	P07737	8.48/8.53	15.22/25.17	9	62	4.30E-52	3
76	Adenine phosphoribosyltransferase	P07741	5.78/5.66	19.77/34.90	6	32	5.40E-24	3
77	Heat shock protein HSP 90-alpha	P07900	ND	ND	ND	ND	3.50E-42	6
78	Heterogeneous nuclear ribonucleoproteins C1/C2	P07910	4.95/8.19	33.71/65.31	7	25	5.50E-03	2
79	Heat shock 70 kDa protein 1	P08107	5.48/6.18	70.29/78.53	17	26	2.30E-47	5
80	Annexin A6	P08133	5.42/6.02	76.17/132.77	41	65	6.80E-63	3
81	Beta-glucuronidase precursor	P08236	6.54/6.94	75.01/132.90	9	24	8.00E-03	1

ID No.	Protein Name	Swiss Prot Access. no. <sup>a</sup>	Theoret./observ. p <sup>b</sup>	Theoret./Observ. Mr <sup>c</sup> (kDa)	Pept. Match (n)	Seq. cov. <sup>d</sup> (%)	Mascot expect. score <sup>e</sup>	Sub. cell. Fract. No. <sup>f</sup>
82	Heat shock protein HSP 90-beta	P08238	4.97/5.38	83.55/154.23	24	35	1.10E-20	1
83	Leukocyte elastase precursor	P08246	9.71/5.65	29.13/70.56	7	34	2.30E-07	3
84	Glutathione S-transferase A1	P08263	ND	ND	ND	ND	6.10E-18	6
85	Vimentin	P08670	5.06/5.24	5.38/86.36	25	57	6.80E-29	5
86	Guanine nucleotide-binding protein G(k) subunit alpha	P08754	ND	ND	ND	ND	2.60E-03	6
87	Annexin A5	P08758	4.94/5.40	35.97/63.04	18	57	6.80E-79	3
88	40S Ribosomal protein SA	P08865	4.79/5.11	32.95/75.93	10	45	1.30E-14	3
89	Glutathione S-transferase P	P09211	5.43/6.01	23.44/37.00	11	53	5.40E-53	1
90	High mobility group protein B1	P09429	5.62/6.56	25.05/57.42	11	46	1.10E-36	3
91	Fructose-1,6-bisphosphatase 1	P09467	6.54/6.75	37.19/74.75	20	54	1.30E-65	3
92	Annexin A4	P09525	5.84/5.97	36.09/61.14	22	63	6.80E-57	1
93	Heterogeneous nuclear ribonucleoprotein A1	P09651	9.26/9.08	38.81/51.48	15	46	3.40E-11	5
94	U2 small nuclear ribonucleoprotein A	P09661	8.72/8.52	28.51/44.45	8	28	7.80E-04	6
95	Leukotriene A-4 hydrolase	P09960	5.80/6.23	69.87/125.95	27	51	1.70E-34	1
96	Histone H2A.Z	P0C085	10.58/5.63	35.67/25.67	2	12	4.40E-06	3
97	Eosinophil-derived neurotoxin	P10153	9.10/8.89	18.86/28.78	5	22	2.30E-24	1
98	Lysosomal alpha-glucosidase precursor	P10253	5.62/5.89	106.13/41.83	13	15	1.00E-03	4
99	Thioredoxin	P10599	4.82/5.31	12.01/17.70	8	55	5.40E-11	1
100	Lysosomal protective protein precursor	P10619	6.16/5.20	54.94/55.37	8	14	9.20E-13	5
101	Esterase D	P10768	6.54/6.57	31.96/56.58	11	49	7.30E-14	1
102	78 kDa glucose-regulated protein precursor	P11021	ND	ND	ND	ND	3.00E-38	6
103	Heat shock cognate 71 kDa protein	P11142	5.37/5.85	71.08/142.38	22	35	9.20E-62	3
104	Integrin alpha-M precursor	P11215	6.88/6.85	128.41/234.21	30	56	1.83E-21	4
105	Medium-chain specific acyl-CoA dehydrogenase, mitochondrial precursor	P11310	8.61/6.84	47.01/80.06	13	35	7.30E-11	3
106	Glucose-6-phosphate 1-dehydrogenase	P11413	6.39/6.88	59.68/112.14	32	70	2.90E-28	3
107	Eosinophil peroxidase precursor	P11678	10.31/7.62	81.96/113.08	13	18	4.60E-07	6
108	Proliferating cell nuclear antigen	P12004	4.57/5.12	29.09/64.84	7	31	3.80E-05	3
109	Annexin A3	P12429	5.63/8.74	36.52/68.97	10	36	1.10E-37	4
110	Eosinophil cationic protein precursor	P12724	10.31/9.53	18.94/35.5	7	42	1.20E-20	3



ID No.	Protein Name	Swiss Prot Access. no. <sup>a</sup>	Theoret./observ. p <sup>b</sup>	Theoret./Observ. Mr <sup>c</sup> (kDa)	Pept. Matic h (n)	Seq. cov. <sup>d</sup> (%)	Mascot score <sup>e</sup>	Sub. cell. Fract. No. <sup>f</sup>
111	Alpha-actinin-1	P12814	5.25	103.56	25	35	1.50E-14	2
112	Myosin heavy chain, cardiac muscle beta isoform	P12883	5.63/3.60	223.76/32.64	17	13	3.00E-03	6
113	ATP-dependent DNA helicase 2 subunit 1	P12956	6.23/6.59	70.08/135.42	22	49	8.50E-42	3
114	Ribonuclease inhibitor	P13489	4.71/5.11	51.77/85.58	21	62	5.40E-56	1
115	Elongation factor 2	P13639	ND	ND	ND	ND	1.40E-16	6
116	Keratin, type I cytoskeletal 10	P13645	5.13/7.93	59.71/150.00	19	29	7.30E-33	3
117	Protein disulfide-isomerase A4 precursor	P13667	4.96/5.51	73.23/143.51	34	48	5.80E-46	3
118	Translationally-controlled tumor protein	P13693	4.84/5.25	19.70/39.23	10	47	1.50E-19	1
119	Delta-aminolevulinic acid dehydratase	P13716	6.32/6.57	36.73/70.58	11	34	5.50E-09	3
120	Bone marrow proteoglycan precursor	P13727	6.23/9.39	25.90/20.82	6	26	1.10E-14	1
121	Plastin-2 (L-plastin)	P13796	5.20/5.63	70.82/121.32	30	57	5.40E-56	1
122	Acylamino-acid-releasing enzyme	P13798	5.29/5.71	82.14/152.88	19	31	4.60E-18	3
123	Macrophage migration inhibitory factor	P14174	8.24/7.90	12.64/18.94	5	24	2.70E-11	1
124	Hematopoietic lineage cell-specific protein	P14317	4.74/7.11	50.08/73.33	8	17	2.20E-04	6
125	Farnesyl pyrophosphate synthetase	P14324	ND	ND	ND	ND	1.70E-08	6
126	Alcohol dehydrogenase [NADP+]	P14550	6.32/6.66	36.89/71.94	18	55	3.40E-40	1
127	Neutrophil cytosol factor 1	P14598	9.12/7.87	44.88/101.38	11	31	7.30E-21	6
128	Pyruvate kinase isozymes M1/M2	P14618	7.96/7.90	58.47/104.26	19	42	5.40E-13	1
129	Endoplasmin precursor	P14625	4.76/5.21	92.67/180.61	28	38	3.60E-56	3
130	Heterogeneous nuclear ribonucleoprotein L	P14866	6.65/6.86	60.72/122.75	12	27	4.60E-08	3
131	Aspartyl-tRNA synthetase, cytoplasmic	P14868	6.11	57.5	22	44	9.98E-24	6
132	Ras-related C3 botulinum toxin substrate 2 precursor	P15153	7.52/7.87	21.81/37.71	8	39	3.60E-44	1
133	Ezrin	P15311	5.94	69.48	20	30	3.15E-19	6
134	Nucleoside diphosphate kinase A	P15531	5.83/6.16	17.31/29.25	6	42	1.80E-16	1
135	Arachidonate 15-lipoxygenase	P16050	6.14/6.58	75.50/114.56	21	40	3.40E-19	1
136	Histone H2A.x	P16104	10.74/5.55	15.14/27.56	4	48	5.80E-04	3
137	Carbonyl reductase [NADPH] 1	P16152	8.55/9.67	30.64/49.27	8	41	2.00E-04	6
138	Beta-galactosidase-related protein precursor	P16279	6.5/6.23	60.86/123.48	11	24	4.60E-11	3
139	Stathmin	P16949	5.76/6.01	17.29/28.28	9	42	2.10E-26	3

ID No.	Protein Name	Swiss Prot Access. no. <sup>a</sup>	Theoret./observ. p <sup>b</sup>	Theoret./Observ. Mr <sup>c</sup> (kDa)	Pept. Matic h (n)	Seq. cov. <sup>d</sup> (%)	Mascot expect. score <sup>e</sup>	Sub. cell. Fract. No. <sup>f</sup>
140	Galectin-3	P17931	8.61/8.20	26.23/57.44	5	22	4.30E-03	1
141	T-complex protein 1 subunit alpha	P17987	ND	ND	ND	ND	3.90E-04	6
142	Vinculin	P18206	5.50/6.47	124.29/176.11	38	36	1.30E-32	1
143	Phosphoglycerate mutase 1	P18669	6.67/6.54	28.90/53.87	14	56	4.30E-31	1
144	Myosin regulatory light chain 2, nonsarcomeric	P19105	4.67/5.04	19.84/30.71	9	63	1.70E-23	2
145	Neutrophil cytosol factor 2	P19878	5.88/6.22	60.24/119.95	21	42	9.20E-23	1
146	Annexin A7	P20073	5.52/6.26	52.99/86.00	10	23	2.30E-09	1
147	Azurocidin precursor	P20160	9.75/9.47	27.32/57.23	5	30	1.70E-13	3
148	Proteasome subunit beta type 1	P20618	8.27/7.84	26.70/43.24	10	52	2.90E-17	3
149	Lamin-B1	P20700	ND	ND	ND	ND	1.70E-21	6
150	Vacuolar ATP synthase subunit B, brain isoform	P21281	5.57/6.03	56.81/101.80	10	25	1.80E-08	3
151	Iron-responsive element-binding protein 1	P21399	ND	ND	ND	ND	1.40E-06	6
152	Voltage-dependent anion-selective channel protein 1	P21796	8.62/5.30	30.87/51.41	9	41	2.10E-19	4
153	Ubiquitin-like modifier-activating enzyme 1	P22314	5.49/5.74	118.86/171.81	29	40	7.30E-30	1
154	Nucleoside diphosphate kinase B	P22392	8.52/8.39	17.40/26.76	13	87	2.30E-28	1
155	Heterogeneous nuclear ribonucleoproteins A2/B1	P22626	8.97/7.79	37.46/45.38	16	42	3.60E-30	3
156	Cytochrome b-c1 complex subunit 2, mitochondrial precursor	P22695	8.74/7.67	48.58/81.54	9	30	4.60E-06	3
157	Liver carboxylesterase 1 precursor	P23141	6.15/6.11	62.77/95.84	13	26	2.80E-05	4
158	Splicing factor, proline- and glutamine-rich	P23246	9.45/7.89	76.21/228.51	9	17	2.90E-20	6
159	Peptidyl-prolyl cis-trans isomerase B precursor	P23284	9.33/9.23	22.79/25.86	7	41	1.80E-09	6
160	Tryptophanyl-tRNA synthetase	P23381	5.83/6.25	53.47/98.77	18	50	4.30E-24	1
161	Adenosylhomocysteinase	P23526	5.92/6.28	48.26/80.14	20	43	2.10E-36	1
162	Cofilin-1	P23528	8.22/8.13	18.72/28.60	10	65	3.40E-26	1
163	Myeloblastin precursor	P24158	8.72/9.04	28.25/25.26	3	11	4.60E-14	4
164	Proteasome subunit alpha type 1	P25786	6.15/6.45	29.82/61.79	10	47	2.90E-16	3
165	Proteasome subunit alpha type 2	P25787	6.92/6.82	26.00/45.64	13	61	1.70E-34	3

ID No.	Protein Name	Swiss Prot Access. no. a	Theoret./observ. p/b	Theoret./Observ. Mr <sup>c</sup> (kDa)	Pept. Matic h (n)	Seq. cov. d (%)	Mascot expect. score <sup>e</sup>	Sub. cell. Fract. No. f
166	Proteasome subunit alpha type 4	P25789	7.57/7.57	29.75/59.21	13	59	4.60E-33	3
167	Moessin	P26038	6.08/6.51	67.89/150.87	30	50	4.30E-51	3
168	Protein S100-A4	P26447	5.85/5.87	11.95/13.94	6	36	2.90E-17	1
169	Elongation factor 1-gamma	P26641	6.25	50.43	15	33	3.97E-36	6
170	Annexin A13	P27216	5.47/5.71	35.54/65.47	8	30	3.00E-04	3
171	14-3-3 protein theta	P27348	ND	ND	ND	ND	1.50E-08	6
172	Replication protein A 70 kDa	P27694	6.92/6.93	68.72/144.08	14	30	5.80E-07	3
173	Calreticulin precursor	P27797	4.29/4.77	48.28/134.58	14	44	4.60E-40	3
174	Histone H2A type 1-E	P28001	11.05/6.25	14.10/26.03	7	43	3.40E-20	3
175	Proteasome subunit beta type 8 precursor	P28062	7.63/8.11	30.68/56.66	10	29	2.30E-30	3
176	Proteasome subunit beta type 9 precursor	P28065	4.93/5.25	23.36/38.82	7	40	3.80E-05	3
177	Proteasome subunit alpha type 5	P28066	4.74/5.18	26.57/55.00	8	43	3.50E-06	3
178	Proteasome subunit beta type 4 precursor	P28070	5.72/5.93	29.23/51.19	7	37	1.50E-16	3
179	Mitogen-activated protein kinase 1	P28482	6.53/6.73	41.76/76.16	5	15	6.80E-08	3
180	Grancalcin	P28676	5.02/5.23	24.22/47.52	10	52	2.90E-18	3
181	Tyrosine-protein phosphatase non-receptor type 6	P29350	7.65/6.32	67.92/101.19	15	33	7.30E-34	3
182	Transketolase	P29401	7.58/7.41	68.52/144.42	14	25	2.30E-58	6
183	Endoplasmic reticulum protein ERp29 precursor	P30040	6.77/6.53	29.03/61.97	11	36	7.30E-41	3
184	Peroxiredoxin-6	P30041	6.02/6.49	25.13/40.62	5	21	3.00E-04	1
185	Flavin reductase	P30043	7.13/7.48	22.22/42.00	10	67	1.30E-30	1
186	Peroxiredoxin-5, mitochondrial precursor	P30044	8.85/7.04	23.00/27.77	11	49	4.60E-26	1
187	Thioredoxin-dependent peroxidase reductase, mitochondrial precursor	P30048	7.67/6.06	28.02/35.25	5	21	5.80E-21	2
188	UMP-CMP kinase	P30085	5.44/5.82	22.44/37.00	9	58	2.90E-08	1
189	Phosphatidylethanolamine-binding protein 1	P30086	7.42/7.63	21.16/35.70	13	67	6.80E-34	1
190	Protein disulfide-isomerase A3 precursor	P30101	5.98/5.95	57.46/108.29	26	49	1.80E-60	3
191	Ser/Thr-protein phosphatase 2A 65 kDa	P30153	4.96/5.51	66.07/121.85	18	35	1.10E-16	3
192	Ser/Thr Sorcin	P30626	5.32/5.49	21.95/33.15	7	40	3.60E-11	2
193	Ser/Thr Leukocyte elastase inhibitor	P30740	5.90/6.20	42.83/74.25	13	38	1.30E-05	2

ID No.	Protein Name	Swiss Prot Access. no. <sup>a</sup>	Theoret./observ. p <sup>b</sup>	Theoret./Observ. Mr <sup>c</sup> (kDa)	Pept. Matic h (n)	Seq. cov. <sup>d</sup> (%)	Mascot expect. score <sup>e</sup>	Sub. cell. Fract. No. <sup>f</sup>
194	Succinate dehydrogenase mitochondrial precursor	P31040	7.06/5.83	73.67/33.63	12	19	1.10E-05	4
195	Coronin-1A	P31146	6.25/6.76	51.68/98.51	14	32	5.40E-08	1
196	Rab GDP dissociation inhibitor alpha	P31150	5.00/5.37	51.12/113.09	22	55	4.60E-22	3
197	Heterogeneous nuclear ribonucleoprotein H3	P31942	6.37/5.73	36.96/69.00	6	26	1.80E-14	6
198	Heterogeneous nuclear ribonucleoprotein H	P31943	5.89	49.48	10	33	3.15E-09	6
199	14-3-3 protein beta/alpha	P31946	4.76/4.09	28.05/59.13	8	32	5.60E-03	6
200	Stress-induced-phosphoprotein 1	P31948	ND	ND	ND	ND	1.40E-04	6
201	Protein S100-A11	P31949	6.51/7.33	10.88/15.94	9	60	5.40E-31	6
202	Peroxiredoxin-2	P32119	5.68/5.46	22.65/36.44	7	27	3.40E-22	2
203	Cytidine deaminase	P32320	6.55/6.16	16.69/24.75	5	48	6.80E-06	2
204	N-acetylgalactosamine-6-sulfatase precursor	P34059	6.25/6.42	58.45/135.28	13	24	5.40E-26	4
205	Heat shock 70 kDa protein 4	P34932	5.18/5.22	95.10/175.14	17	20	3.60E-07	3
206	Prohibitin	P35232	5.57/7.38	29.84/61.79	5	24	4.20E-03	4
207	Keratin, type I cytoskeletal 9	P35527	5.19/5.72	62.32/122.35	15	35	1.20E-14	3
208	Phosphoenolpyruvate carboxykinase, cytosolic [GTP]	P35558	ND	ND	ND	ND	8.70E-45	6
209	Myosin-9	P35579	5.50/5.51	227.65/214.11	33	23	2.10E-12	2
210	Myosin-11	P35749	5.42/5.77	228.05/131.40	25	16	3.10E-04	2
211	Keratin, type II cytoskeletal 2 epidermal	P35908	8.07/6.14	66.11/43.76	12	22	2.90E-12	1
212	Phosphoglucomutase-1	P36871	6.32/6.48	61.56/105.99	21	43	3.60E-20	1
213	Phospholipid hydroperoxide glutathione peroxidase, mitochondrial precursor	P36969	8.64/7.50	22.68/29.12	11	60	9.20E-20	1
214	Hippocalcin-like protein 1	P37235	5.21/5.36	22.41/31.71	6	32	2.10E-05	1
215	Transgelin-2	P37802	8.41/8.07	22.55/35.68	17	75	5.40E-35	1
216	Transaldolase	P37837	6.36/5.89	37.69/63.54	18	45	2.30E-38	4
217	Vacuolar ATP synthase catalytic subunit A, ubiquitous isoform	P38606	5.35/5.72	68.66/137.78	15	32	6.80E-09	3
218	Stress-70 protein, mitochondrial precursor	P38646	5.87/5.80	73.92/131.24	18	32	2.90E-37	3
219	Eukaryotic initiation factor 4A-III	P38919	6.30/6.43	47.13/88.36	7	14	3.40E-12	3
220	Acidic leucine-rich nuclear phosphoprotein 32	P39687	3.99/4.48	28.68/56.85	9	31	1.80E-18	3

ID No.	Protein Name	Swiss Prot Access. no. <sup>a</sup>	Theoret./observ. pI <sup>b</sup>	Theoret./Observ. Mr <sup>c</sup> (kDa)	Pept. Matic h (n)	Seq. cov. <sup>d</sup> (%)	Mascot expect. score <sup>e</sup>	Sub. cell. Fract. No. <sup>f</sup>
221	Macrophage capping protein	P40121	5.88/6.17	38.78/75.25	11	43	2.30E-07	1
222	Malate dehydrogenase, cytoplasmic	P40925	ND	ND	ND	ND	6.90E-15	6
223	Malate dehydrogenase, mitochondrial precursor	P40926	8.92/9.11	35.96/61.23	13	50	1.50E-14	6
224	Myeloid cell nuclear differentiation antigen	P41218	9.77/7.92	46.09/111.49	8	23	1.80E-19	6
225	Tyrosine-protein kinase CSK	P41240	6.62/6.92	51.24/99.43	15	44	2.90E-10	3
226	Caspase-3 precursor	P42574	6.09/6.50	32.04/56.82	19	63	5.80E-21	2
227	Lysosomal Pro-X carboxypeptidase precursor	P42785	6.75/6.47	56.28/109.73	14	26	2.30E-21	4
228	Platelet-activating factor acetylhydrolase IB subunit alpha	P43034	6.97	47.18	13	34	9.98E-25	6
229	Glycerol-3-phosphate dehydrogenase, mitochondrial precursor	P43304	7.23	81.3	20	26	3.97E-14	6
230	26S protease regulatory subunit 6B	P43686	ND	ND	ND	ND	4.00E-04	6
231	Ubiquitin carboxyl-terminal hydrolase 5	P45974	4.91/5.42	96.64/168.41	19	25	3.60E-07	1
232	Crk-like protein	P46109	6.26/6.47	33.87/67.18	14	57	7.30E-11	2
233	Vesicle-fusing ATPase	P46459	6.52	83.02	17	24	1.26E-07	6
234	F-actin capping protein subunit beta	P47756	5.36/5.88	31.62/57.61	19	65	2.10E-27	2
235	26S proteasome non-ATPase regulatory subunit 8	P48556	6.85/6.51	30.16/52.13	11	33	4.30E-20	2
236	Serpine B10	P48595	5.80/5.97	45.49/241.04	21	59	3.60E-42	1
237	Glutathione synthetase	P48637	ND	ND	ND	ND	5.50E-15	6
238	T-complex protein 1 subunit epsilon	P48643	ND	ND	ND	ND	3.00E-04	6
239	Keratin, type II cytoskeletal 6E	P48668	8.14/6.99	60.27/44.52	16	29	2.10E-09	2
240	Isocitrate dehydrogenase [NADP], mitochondrial precursor	P48735	8.88/6.53	51.33/116.03	20	47	1.50E-19	4
241	CD97 antigen precursor	P48960	6.50/5.39	94.60/133.76	7	9	9.20E-07	2
242	Calcium signal-modulating cyclophilin ligand	P49069	ND	ND	ND	ND	9.30E-06	6
243	Ribose-5-phosphate isomerase	P49247	8.78/7.18	33.53/54.80	8	27	4.30E-11	1
244	T-complex protein 1 subunit gamma	P49368	6.10/6.42	61.07/109.15	16	33	4.60E-12	2
245	Elongation factor Tu, mitochondrial precursor	P49411	7.26	49.85	8	23	9.98E-06	6
246	Proteasome subunit beta type 3	P49720	6.14/6.31	23.22/48.25	11	50	1.50E-23	3

ID No.	Protein Name	Swiss Prot Access. no. <sup>a</sup>	Theoret./observ. pI <sup>b</sup>	Theoret./Observ. Mr <sup>c</sup> (kDa)	Pept. Matic h (n)	Seq. cov. <sup>d</sup> (%)	Mascot score <sup>e</sup>	Sub. cell. Fract. No. <sup>f</sup>
247	Proteasome subunit beta type 2	P49721	6.51	22.99	10	46	2.51E-19	6
248	Rab GDP dissociation inhibitor beta	P50395	6.11/6.37	51.09/82.02	30	73	9.20E-59	1
249	Vasodilator-stimulated phosphoprotein	P50552	9.05/6.34	39.98/56.07	8	23	8.50E-11	4
250	Dynamin-2	P50570	7.04/6.38	98.45/131.31	24	29	1.80E-18	3
251	Annexin A11	P50995	7.53/8.48	54.68	24	41	1.50E-40	4
252	Ras-related protein Rab-5C	P51148	8.64/5.23	23.70/56.07	9	44	4.40E-06	4
253	Ras-related protein Rab-7	P51149	6.4	23.76	12	66	6.80E-37	3
254	Ras-related protein Rab-27A	P51159	5.19/5.50	25.13/52.12	9	35	4.60E-10	2
255	Galactokinase	P51570	6.04/5.90	42.70/77.82	11	28	1.50E-38	6
256	Heterogeneous nuclear ribonucleoprotein A3	P51991	9.10/9.66	39.80/63.97	11	31	2.80E-04	6
257	6-phosphogluconate dehydrogenase	P52209	6.80/7.07	53.62/83.71	21	46	6.80E-51	1
258	Heterogeneous nuclear ribonucleoprotein M	P52272	8.85/8.12	77.62/79.83	16	26	9.30E-04	6
259	Rho GDP-dissociation inhibitor 1	P52565	5.03/5.43	23.25/51.19	10	43	1.10E-32	3
260	Rho GDP-dissociation inhibitor 2	P52566	5.10/5.61	23.03/49.74	12	80	6.80E-19	3
261	Hexokinase-3	P52790	5.27/5.57	100.51/166.43	20	26	2.30E-21	1
262	F-actin capping protein alpha-1 subunit	P52907	5.45/5.74	33.07/64.26	16	69	1.70E-15	2
263	Biliverdin reductase A precursor	P53004	6.06/6.35	33.69/69.46	13	42	5.80E-34	1
264	ATP-citrate synthase	P53396	6.95/7.17	121.66/214.05	34	39	9.20E-30	3
265	Dipeptidyl-peptidase 1 precursor	P53634	6.54/5.37	52.61/21.11	5	10	8.70E-05	3
266	Tyrosyl-tRNA synthetase, cytoplasmic	P54577	6.64/6.84	56.45/116.20	13	27	5.40E-10	3
267	Adenylate kinase isoenzyme 2, mitochondrial	P54819	7.85/8.25	26.69/55.06	9	41	8.50E-11	4
268	Alpha-soluble NSF attachment protein	P54920	5.23/5.57	33.68/63.46	12	44	4.60E-12	3
269	Transitional endoplasmic reticulum ATPase	P55072	ND	ND	ND	ND	6.60E-05	6
270	Histone H2B type 1-D	P58876	10.32/9.56	13.98/27.17	7	52	1.10E-11	3
271	Neutrophil defensin 1 precursor	P59665	6.54/8.33	10.54/55.89	5	26	4.60E-17	4
272	Actin-related protein 2/3 complex subunit 4	P59998	8.53/8.48	19.67/31.69	10	44	3.60E-16	3
273	Triosephosphate isomerase	P60174	6.45/6.82	26.94/47.85	16	70	2.30E-42	1
274	Myosin light polypeptide 6	P60660	4.56/3.51	16.96/18.16	10	62	4.30E-24	6
275	Actin, cytoplasmic 1	P60709	5.29/5.8	42.02/63.77	6	23	7.30E-21	2

ID No.	Protein Name	Swiss Prot Access. no. a	Theoret./observ. p <sup>b</sup>	Theoret./Observ. Mr <sup>c</sup> (kDa)	Pept. Matic h (n)	Seq. cov. d (%)	Mascot expect. score <sup>e</sup>	Sub. cell. Fract. No. f
276	Eukaryotic initiation factor 4A-I	P60842	5.32/5.8	46.35/92.56	18	50	1.20E-09	3
277	Ribose-phosphate pyrophosphokinase I	P60891	6.56/6.94	35.33/68.86	8	28	1.70E-07	3
278	Proteasome subunit alpha type 6	P60900	6.34/6.47	27.84/50.00	7	31	2.90E-09	3
279	Cell division control protein 42 homolog precursor	P60953	5.76/6.85	21.70/34.13	6	29	9.20E-15	3
280	Dextrin	P60981	8.06/7.95	18.95/28.60	1	6	2.30E-03	3
281	Ras-related protein Rab-2A	P61019	6.08/5.83	23.70/47.74	9	50	5.80E-11	3
282	Ubiquitin-conjugating enzyme E2 N	P61088	6.13/6.22	17.18/25.71	11	57	9.20E-15	1
283	Actin-related protein 3	P61158	5.61/6.12	47.67/84.00	17	48	6.80E-40	1
284	Actin-like protein 2	P61160	6.30/6.58	45.02/79.74	17	50	3.60E-17	3
285	Alpha-centractin	P61163	6.19	42.7	12	37	1.80E-16	2
286	ADP-ribosylation factor 3	P61204	6.84/7.07	20.46/56.97	11	69	5.40E-16	4
287	Ras-related protein Rap-1b precursor	P61224	5.65/5.82	21.04/57.68	8	43	1.50E-10	4
288	Transforming protein RhoA precursor	P61586	5.83/6.34	22.10/42.90	8	39	2.30E-11	1
289	10 kDa heat shock protein, mitochondrial	P61604	8.91/6.94	10.92/169.95	9	66	6.80E-26	4
290	Lysozyme C precursor	P61626	9.38/8.95	16.98/23.91	6	38	7.30E-12	1
291	Beta-2-microglobulin precursor	P61769	6.06/6.43	13.82/28.62	3	37	3.40E-04	4
292	Heterogeneous nuclear ribonucleoprotein K	P61978	5.39/5.88	51.30/107.85	14	34	1.80E-12	2
293	14-3-3 protein gamma	P61981	4.8	28.46	9	36	3.40E-10	2
294	Ser/Thr protein phosphatase alpha catalytic subunit	P62136	5.94/6.15	38.23/71.15	14	32	7.30E-18	3
295	Ser/Thr protein phosphatase beta catalytic subunit	P62140	5.84/6.18	37.69/72.20	17	58	1.30E-12	3
296	Calmodulin	P62158	4.09/3.38	16.70/23.48	5	45	1.10E-19	6
297	14-3-3 protein epsilon	P62258	4.63	29.33	13	53	2.30E-18	3
298	26S protease regulatory subunit S10B	P62333	7.1	44.43	12	35	5.00E-09	6
299	Ras-related protein Rab-11A	P62491	3.12/8.88	24.49/28.69	9	33	4.90E-06	4
300	Histone H4	P62805	11.36/9.50	11.36/24.82	7	56	3.40E-33	3
301	Histone H2B type 1-C/E/F/G/I	P62807	10.31/8.47	13.98/26.16	9	61	4.30E-21	3
302	GTP-binding nuclear protein Ran	P62826	7.01/7.14	24.57/43.15	15	56	1.70E-28	1
303	Guanine nucleotide-binding protein G(I)/G(S)/G(T) subunit beta 2	P62879	5.60/5.87	38.05/67.26	8	32	2.00E-03	3

ID No.	Protein Name	Swiss Prot Access. no. a	Theoret./observ. pI <sup>b</sup>	Theoret./Observ. Mr <sup>c</sup> (kDa)	Pept. Matic h (n)	Seq. cov. d (%)	Mascot expect. score <sup>e</sup>	Sub. cell. Fract. No. f
304	Peptidyl-prolyl cis-trans isomerase A	P62937	7.68/8.09	18.23/27.67	11	61	4.30E-46	1
305	FK506-binding protein 1A	P62942	7.88/8.05	12.00/20.77	6	50	6.80E-12	1
306	Ubiquitin	P62988	6.56/6.97	8.56/23.81	6	61	2.30E-24	3
307	Growth factor receptor-bound protein 2	P62993	5.89/6.2	25.30/47.79	15	61	9.20E-32	2
308	14-3-3 protein zeta/delta	P63104	4.73/5.31	27.90/53.92	14	56	2.30E-42	3
309	Eukaryotic translation initiation factor 5A-1	P63241	5.08/5.63	17.05/29.02	6	45	6.00E-04	3
310	Guanine nucleotide-binding protein subunit beta 2-like 1	P63244	7.56/7.56	35.51/63.97	18	70	4.30E-33	3
311	Actin, cytoplasmic 2	P63261	5.31/5.80	42.11/76.93	17	46	3.60E-57	1
312	Ser/Thr protein phosphatase 2A catalytic subunit alpha isoform	P67775	5.30/5.76	36.14/70.58	10	45	3.30E-06	3
313	Elongation factor 1-alpha 1	P68104	9.10/7.87	50.45/106.51	7	19	1.50E-19	6
314	Tubulin alpha-ubiquitous chain	P68363	4.94/5.99	50.80/87.80	13	39	4.60E-07	2
315	Tubulin beta-2C chain	P68371	4.79/5.59	50.26/95.91	18	38	1.50E-29	3
316	Histone H3.1	P68431	11.27/8.58	15.44/27.15	4	20	2.70E-07	3
317	Hemoglobin subunit beta	P68871	6.75/7.05	16.10/19.88	13	89	4.30E-79	1
318	Hemoglobin subunit alpha	P69905	8.72/8.49	15.31/233.09	6	62	2.70E-34	1
319	T-complex protein 1 subunit beta	P78371	6.01	57.79	14	42	6.29E-10	6
320	Glutathione transferase omega-1	P78417	6.23/6.36	27.83/52.67	16	46	7.30E-35	1
321	Neutrophil gelatinase-associated lipocalin Precursor	P80188	9.02/8.04	22.74/41.77	12	63	1.20E-17	4
322	Protein S100-A12	P80511	5.83/6.30	10.57/11.87	6	45	1.70E-21	1
323	Nuclear protein Hcc-1	P82979	6.13/6.46	23.71/59.89	4	18	2.30E-03	3
324	ADP-ribosylation factor 1	P84077	6.32/6.31	20.70/29.64	11	69	8.50E-16	3
325	Histone H3.3	P84243	11.27/7.29	15.38/26.42	8	44	2.10E-14	3
326	Sorbitol dehydrogenase	Q00796	8.25/9.59	38.90/63.57	12	36	2.80E-05	6
327	Adenyl cyclase-associated protein 1	Q01518	8.12/6.70	52.22/109.94	8	27	6.80E-17	6
328	Lactoylglycyl-L-homoserine kinase	Q04760	5.12/5.38	20.99/35.44	6	32	1.00E-03	1
329	Galectin-10	Q05315	6.82/7.15	16.58/20.60	6	66	1.10E-11	1
330	Proteasome activator complex subunit 1	Q06323	5.78/6.14	28.88/59.02	15	61	1.80E-30	3
331	Peroxiredoxin-1	Q06830	8.27/8.26	22.32/40.87	18	75	2.30E-64	1



ID No.	Protein Name	Swiss Prot Access. no. <sup>a</sup>	Theoret./observ. p <sup>b</sup>	Theoret./Observ. Mr <sup>c</sup> (kDa)	Pept. Match (n)	Seq. cov. <sup>d</sup> (%)	Mascot expect. score <sup>e</sup>	Sub. cell. Fract. No. <sup>f</sup>
332	Splicing factor, arginine/serine-rich 1	Q07955	10.37/6.40	27.84/68.78	9	38	4.80E-05	3
333	Rho-GTPase-activating protein 1	Q07960	5.85/6.34	50.46/96.08	21	57	1.80E-25	3
334	Secemin-1	Q12765	4.66/5.14	46.80/10.21	12	29	9.20E-07	3
335	Nuclear pore complex protein Nup160	Q12769*	5.41/9.17	151.13/83.21	12	12	4.60E-03	3
336	Delta(3,5)-Delta(2,4)-dienoyl-CoA isomerase	Q13011	8.16	36.14	7	25	2.51E-06	6
337	Ubiquitin-conjugating enzyme E2 variant 1	Q13404	8.56/6.07	26.07/55.70	8	32	4.60E-07	4
338	Dynaactin subunit 2	Q13561	5.10/5.30	44.19/52.24	10	35	1.70E-06	6
339	NEDD8-activating enzyme E1 subunit	Q13564	ND	ND	ND	ND	1.20E-04	6
340	Spectrin alpha chain, brain	Q13813	5.22/5.55	285.16/203.12	40	23	7.30E-18	2
341	Spliceosome RNA helicase BAT1	Q13838	5.44/5.99	49.42/95.04	15	35	9.20E-18	3
342	Coactosin-like protein	Q14019	5.54/6.69	16.05/25.85	12	57	3.40E-19	4
343	Heterogeneous nuclear ribonucleoprotein D0	Q14103	7.62/5.93	38.58/91.86	7	22	5.20E-05	4
344	Septin-6	Q14141	6.24	50.08	17	35	7.92E-08	6
345	Keratin, type I cuticular Ha3-II	Q14525	4.81/5.77	47.33/192.32	14	44	1.50E-12	2
346	Neutral alpha-glucosidase AB precursor	Q14697	5.74/6.21	107.26/196.40	24	28	9.20E-13	3
347	Major vault protein	Q14764	5.34/5.86	99.55/174.43	19	22	1.70E-11	2
348	LIM and SH3 domain protein 1	Q14847	6.61/6.81	30.10/71.22	10	33	1.80E-11	3
349	Orphan nuclear receptor NRII3	Q14994	ND	ND	ND	ND	2.50E-03	6
350	Septin-2	Q15019	6.15/6.48	41.69/72.94	7	26	1.60E-04	2
351	Neutrophil cytosol factor 4	Q15080	6.40/6.49	39.12/74.10	8	26	1.80E-11	2
352	Protein disulfide-isomerase A6 precursor	Q15084	4.95/5.42	48.90/88.78	15	43	2.90E-15	3
353	Poly(rC)-binding protein 1	Q15365	6.66	37.99	7	30	3.97E-08	6
354	Ras suppressor protein 1	Q15404	8.57/8.54	31.52	16	56	1.10E-27	3
355	Protein phosphatase 1 regulatory subunit 7	Q15435	4.84/5.39	41.65	10	32	3.90E-06	3
356	Syntaxin-binding protein 2	Q15833	6.11/6.45	66.85	13	33	1.80E-09	3
357	Ras-related protein Rab-11B	Q15907	5.65/5.80	24.59	9	40	2.70E-24	3
358	Histone H2A type 2-C	Q16777	10.90/6.70	14.00/26.34	4	49	7.80E-04	3
359	Short chain 3-hydroxyacyl-CoA dehydrogenase, mitochondrial precursor	Q16836	8.88/5.86	34.21/27.24	10	38	1.80E-18	4
360	Thioredoxin reductase 1, cytoplasmic	Q16881	6.07	55.47	11	27	1.58E-08	6

ID No.	Protein Name	Swiss Prot Access. no. <sup>a</sup>	Theoret./observ. p <sup>b</sup>	Theoret./Observ. Mr <sup>c</sup> (kDa)	Pept. Match (n)	Seq. cov. <sup>d</sup> (%)	Mascot score <sup>e</sup>	Sub. cell. Fract. No. <sup>f</sup>
precursor								
361	Chaperonin containing TCP1, subunit 8	Q53HU0	ND	ND	ND	ND	1.40E-05	6
362	This TrEMBL entry deleted	Q5JV65	ND	ND	ND	ND	4.80E-26	6
363	Histone H2B type 2-F	Q5QNW6	10.31/9.82	13.98/27.27	8	61	5.80E-20	3
364	Twinfilin-2	Q6IBS0	6.37/6.71	39.75/79.74	10	42	4.60E-07	3
365	NAPRT Protein	Q6PIL1	ND	ND	ND	ND	5.50E-24	6
366	Staphylococcal nuclease domain-containing protein 1	Q7KZF4	6.74/6.92	102.62/200.89	21	27	7.30E-14	3
367	Histone H2A type 3	Q7L7L0	11.05/5.96	14.10/25.95	5	35	8.50E-21	3
368	Keratin, type II cytoskeletal 1b	Q7Z794	ND	ND	ND	ND	3.00E-11	6
369	Unc-112-related protein 2	Q86UX7	6.52/6.21	76.48/68.65	23	29	4.60E-22	3
370	Ras-related protein Rab-43	Q86YS6	5.44/5.10	23.55/56.43	7	45	5.80E-07	4
371	Dedicator of cytokinesis protein 3	Q8IZD9	6.52/9.18	235.01/33.43	12	7	8.00E-03	6
372	Nesprin-1	Q8NF91	5.38	1011.04	35	6	3.15E-03	6
373	Gamma-glutamyl hydrolase precursor	Q92820	6.67/6.59	36.34/59.02	4	14	4.30E-04	1
374	Probable ATP-dependent RNA helicase DDX17	Q92841	8.82/9.65	72.95/105.93	13	22	8.20E-03	6
375	Histone H2A type 1-C	Q93077	11.05/3.49	14.10/18.34	5	23	6.80E-10	3
376	Histone H2B type 1-H	Q93079	10.31/8.86	13.93/27.11	3	27	5.40E-10	3
377	Uncharacterized protein C19orf10 precursor	Q969H8	6.20/6.16	18.90/53.14	4	27	2.20E-03	4
378	Far upstream element-binding protein 1	Q96AE4	7.18/8.36	67.69/60.93	19	39	2.90E-33	4
379	EF-hand domain-containing protein 2	Q96C19	5.15/5.37	26.79/57.61	23	62	3.60E-28	2
380	Phosphoglucomutase-2	Q96G03	6.28	68.75	19	35	1.26E-09	6
381	ERO1-like protein alpha precursor	Q96HE7	5.48/5.87	55.21/127.76	11	27	2.90E-11	3
382	Abhydrolase domain-containing protein 14B	Q96IU4	5.94/6.05	22.45/36.45	6	38	2.10E-03	1
383	Histone H2A type 1-H	Q96KK5	10.88/7.06	13.93/20.48	5	38	2.70E-08	3
384	Cytosolic nonspecific dipeptidase	Q96KP4	5.66	53.19	12	35	6.29E-04	6
385	RNA-binding protein 14	Q96PK6	9.68/9.71	69.62/102.34	14	25	8.50E-04	6
386	Calponin-2	Q99439	6.92/6.99	34.07/60.59	14	49	1.10E-11	2
387	Synaptic vesicle membrane protein VAT-1 homolog	Q99536	5.88/6.17	42.12/82.48	16	50	4.60E-14	3

ID No.	Protein Name	Swiss Prot Access. no. <sup>a</sup>	Theoret./observ. p <sup>b</sup>	Theoret./Observ. Mr <sup>c</sup> (kDa)	Pept. Matic h (n)	Seq. cov. <sup>d</sup> (%)	Mascot expect. score <sup>e</sup>	Sub. cell. Fract. No. <sup>f</sup>
388	Translin-associated protein X	Q99598	6.10/6.38	33.21/60.00	10	50	1.50E-06	2
389	Monoglyceride lipase	Q99685	6.49/6.18	33.47/67.37	6	24	7.40E-04	4
390	3-hydroxyacyl-CoA dehydrogenase type-2	Q99714	7.66/6.25	27.13/18.90	7	11	3.60E-04	4
391	Aconitate hydratase, mitochondrial precursor	Q99798	7.36/6.76	86.11/52.51	13	20	9.20E-42	4
392	Copine-1	Q99829	5.52/5.92	59.65/119.95	13	24	2.30E-22	1
393	Histone H2A type 1-J	Q99878	10.88/5.71	13.93/25.78	6	38	1.10E-15	3
394	Uncharacterized protein C9orf142	Q9BUH6	5.39/5.60	21.97/38.08	9	42	3.40E-09	2
395	Transmembrane emp24 domain-containing protein 9 precursor	Q9BVK6	6.67/6.57	25.20/40.69	11	55	2.70E-06	2
396	Kinesin light chain 2	Q9H0B6	6.72/6.36	69.29/79.92	14	29	8.20E-03	2
397	Haloacid dehalogenase-like hydrolase domain-containing protein 2	Q9H0R4	ND	ND	ND	ND	1.70E-05	6
398	Ras-related protein Rab-1B	Q9H0U4	5.55/5.64	22.33/41.56	4	20	2.10E-05	3
399	EH domain-containing protein 1	Q9H4M9	6.35	60.65	13	26	9.98E-04	6
400	Sideroflexin-1	Q9H9B4	9.22/5.90	35.88/27.94	10	34	1.30E-05	4
401	Phosphopantothemate--cysteine ligase	Q9HAB8	6.25/6.74	33.98/65.20	8	24	2.00E-06	3
402	Retinoid-inducible serine carboxypeptidase precursor	Q9HB40	5.61/6.34	51.08/26.26	8	15	4.60E-08	1
403	Adipocyte plasma membrane-associated Protein	Q9HDC9	5.82/7.04	46.62/50.00	21	48	2.90E-38	4
404	Exosome complex exonuclease RRP41	Q9NPD3	6.08/6.39	26.65/48.50	9	40	6.60E-04	2
405	Protein FAM49B	Q9NUQ9	5.76/6.03	37.01/60.98	16	49	4.60E-22	1
406	Dipeptidyl-peptidase 3	Q9NY33	5.02/5.37	82.88/153.84	9	12	9.20E-18	3
407	Tropomodulin-3	Q9NYL9	ND	ND	ND	ND	1.20E-29	6
408	EH-domain-containing protein 3	Q9NZN3	6.06/6.44	61.97/50.21	12	24	7.60E-04	2
409	Vacuolar protein sorting 29	Q9UBQ0	6.29/6.70	20.66/35.44	8	43	3.60E-13	2
410	Fructose-1,6-bisphosphate aldolase A [Fragment]	Q9UCN2	ND	ND	ND	ND	7.20E-05	6
411	Protein NipSnap3A	Q9UFN0	9.21/8.65	28.56/37.28	6	25	5.20E-06	6
412	Mitogen-activated protein kinase kinase 1	Q9UHA4	6.73/6.59	13.67/24.23	3	43	3.60E-07	3
413	N-acetylglucosamine kinase	Q9UJ70	5.82/6.11	37.69/70.84	14	44	5.40E-15	2
414	DCC-interacting protein 13 alpha	Q9UKG1	ND	ND	ND	ND	6.90E-08	6

ID No.	Protein Name	Swiss Prot Access. no. <sup>a</sup>	Theoret./observ. <i>p</i> <sup>b</sup>	Theoret./Observ. Mr <sup>c</sup> (kDa)	Pept. Match (n)	Seq. cov. <sup>d</sup> (%)	Mascot expect. score <sup>e</sup>	Sub. cell. Fract. No. <sup>f</sup>
415	Proteasome activator complex subunit 2	Q9UL46	5.44/5.69	27.52/55.19	11	43	5.20E-06	2
416	Apoptosis-associated speck-like protein containing a CARD	Q9ULZ3	5.95/6.54	21.67/38.14	7	37	7.30E-09	1
417	Protein-arginine deiminase type-4	Q9UM07	6.15/6.58	75.13/116.76	9	19	4.60E-08	2
418	NSFL1 cofactor p47	Q9UNZ2	ND	ND	ND	ND	5.50E-17	6
419	RuvB-like 2	Q9Y230	5.49/5.73	51.30/87.80	18	43	5.40E-11	2
420	Cofilin-2	Q9Y281	7.66/7.49	18.84/29.00	5	28	1.50E-03	1
421	Trafficking protein particle complex subunit 4	Q9Y296	5.83/6.24	24.44/40.69	13	60	3.60E-14	2
422	SH3 domain-binding protein 1	Q9Y3L3	6.33/6.44	76.01/139.19	4	5	1.00E-03	2
423	Talin-1	Q9Y490	5.77/6.23	271.77/231.63	47	27	2.90E-45	1
424	Heme-binding protein 2	Q9Y5Z4	4.58/5.81	22.86/69.71	3	18	4.60E-12	3
425	Actin, alpha cardiac muscle 1	P68032	5.23	42.33	4	16	1.58E-03	6
426	High mobility group protein B2	P26583	5.62/7.16	24918.2/44.58	11	43	5.80E-28	4

**Table 2**

## Summary prefractionation protein ID's

Fractions analyzed	Protein IDs	Non-redundant Protein IDs <sup>a</sup>
<b>Subcellular fractions<sup>b</sup></b>		
1-cytoplasm	625	95
2-organelle	425	50
3-nucleus	693	141
4-cytoskeleton	<u>345</u>	<u>52</u>
Total subcellular	2088	338
<b>IEF fractions<sup>c</sup></b>		
pH 3.0–5.4	44	4
pH 5.4–7.0	181	13
pH 7.0–10.0	<u>226</u>	<u>16</u>
Total IEF	451	33
<b>Whole cell lysate</b>	480	63
<b>Total all fractions</b>	3019	434

<sup>a</sup>Had Mascot expectation scores of  $10^{-3}$  or less.

<sup>b</sup>According to Calbiochem's ProteoExtract® Subcellular Proteome Extraction kit.

<sup>c</sup>Using ZOOM® IEF Fractionator (Invitrogen).